1 **Oxalic acid binds to gustatory receptor Gr23a and inhibits feeding in the brown**
2 **planthopper**

3

4 Kui Kang[1,2†], Mengyi Zhang[1†], Lei Yue[1], Weiwen Chen[1], Yangshuo Dai[1], Kai Lin[1],
5 Kai Liu[1], Jun Lv[1], Zhanwen Guan[1], Shi Xiao[1], Wenqing Zhang[1*]

6

7 [1]State Key Laboratory of Biocontrol and School of Life Sciences, Sun Yat-sen
8 University, Guangzhou 510275, Guangdong, China. [2]College of Biology and
9 Agriculture, Zunyi Normal University, Zunyi 563006, Guizhou, China. [†]These authors
10 contributed equally to this work. [*]Corresponding author. Tel: + 86 20 39332963;
11 E-mail: lsszwq@mail.sysu.edu.cn

12

Abstract

Plants produce diverse secondary compounds as natural protection against microbial and insect attack. Most of these compounds, including bitters and acids, are sensed by insect gustatory receptors (Grs). Acids are potentially toxic to insects, but there are few reports on sour compounds as ligands of insect Grs. Here, using two different heterologous expression systems, the insect Sf9 cell line and the mammalian HEK293T cell line, we started from crude extracts of rice (*Oryza sativa*) and successfully identified oxalic acid (OA) as a ligand of NlGr23a, a Gr in the brown planthopper *Nilaparvata lugens*. The antifeedant effect of OA on the brown planthopper was dose dependent, and *NlGr23a* is essential for OA's antifeedant activity in both artificial diets and rice plants. *NlGr23a* is also indispensable for tarsal OA sensing. To our knowledge, OA is the first identified ligand starting from plant crude extracts and the first known strong acid for insect Grs. These findings on rice-planthopper interactions will be of broad interest for pest control in agriculture and also for better understanding of how insects select host plants.

Research organism: *Nilaparvata lugens*

Introduction

Plant visual and chemical cues are important for host location and host acceptance of phytophagous insects. The cabbage root fly, *Delia radicum*, makes use of leaf colors to discriminate among host plants (Prokopy *et al*., 1983). Host selection in oligophagous species is involved with the balance of phagostimulatory and deterrent inputs with the addition of a specific chemical sign stimulus (Chapman, 2003). Understanding the mechanisms underlying this selection strategy is of practical importance in agriculture for pest control. For instance, tandem deployment of the napier grass, which attracts more oviposition by stemborer moths than maize but not suitable for survival, and the molasses grass, which causes over 80% reduction in stemborer infestation of maize, can interfere host selection by stemborers (Khan *et al.*, 2014). The combination of stimuli that have negative effects on food selection by pests and positive effects on diverting pests from the protected resource to a trap can

45 reduce pest abundance on the protected resource, which is called the push-pull

46 strategy (Cook *et al.*, 2007). Plant-derived antifeedants can be used as push

47 components of the push-pull strategy (Cook et al., 2007). Identification of receptors

48 sensing these chemicals will definitely improve our understanding of how insects

49 select host plants.

50 To date, most identified antifeedants are secondary metabolites, which are toxic or

51 deterrent to insects (Yoshihara *et al.*, 1980; Chapman, 2013; Douglas, 2017). As an

52 example, oxalic acid (OA), the simplest dicarboxylic acid common in plant tissues,

53 provides protection for plants against insects and foraging animals, including the

54 brown planthopper (BPH) and aphids (Massonie, 1980; Yoshihara *et al.*, 1980;

55 Karatolos and Hatcher, 2008). Some antifeedants (e.g. tricin) could be even used as

56 indicators of crop resistance to target insect pests, and are therefore potentially

57 valuable for breeding resistant crop varieties (Zhang *et al.*, 2015).

58 In insects, gustatory receptor neurons (GRNs), mainly found in gustatory sensilla,

59 are able to convert the chemical signal into an electrical one, and transmit it to

60 higher-order brain structures for processing, which in turn dictates behaviour (Scott,

61 2018). Secondary compounds as deterrents stimulate a subset of bitter GRNs, which

62 then inhibit feeding activity or induce repulsion (Chapman, 2003). Different

63 secondary metabolites elicited different responding patterns of GRNs in the two

64 *Helicoverpa* species might mediate the dietary acceptance and host range (Sun *et al.*,

65 2021).With the decoding and publication of the genomes of *Drosophila melanogaster*

66 and other insect species, fruitful molecular studies on insect gustation have been

67 enabled. Gustatory receptors (Grs), expressed in GRNs, are required for responses to

68 specific tastants. Grs mainly include sweet, bitter and CO_2 receptors (Liman *et al.*,

69 2014). Although diverse sugars and bitter compounds have been identified as ligands

70 of insect Grs (Chen and Dahanukar, 2020), many Grs have yet to be functionally

71 annotated, particularly the Grs sense acids. DmGr64e in *D. melanogaster* was

72 reported to sense fatty acids such as hexanoic acid and octanoic acid (Kim *et al.*,

73 2018). However, there are currently no reports of strong acid as ligands of insect Grs.

74   The BPH *Nilaparvata lugens*, causing extensive damage by sap feeding and

75   transmitting viruses, feeds solely on cultivated rice and its allied wild forms such as

76   *Oryza perennis* and *O. spontanea* (Sogawa, 1982). Its gustatory sensilla are mainly

77   located in the small passageway leading from the food duct to the cibarium and the

78   stylet groove on the labial tip, and probably regulate the initial stages of probing and

79   in the maintenance of sap ingestion (Foster *et al.*, 1983a; Foster *et al.*, 1983b). In our

80   previous study, 32 of *N. lugens* Gr sequences (*NlGrs*) were obtained following

81   analyses of the BPH genome and transcriptomes (Kang *et al.*, 2018). Here, we

82   selected a functionally unknown gene, *NlGr23a*, which is related to BPH fecundity.

83   Through a multi-stage bioassay-directed fractionation of rice crude extracts, we

84   identified OA as a ligand of NlGr23a. We also found that *NlGr23a* is essential to the

85   antifeedant activity of OA in both artificial diets and rice plants and the modulation of

86   the tarsal repulsion for OA. To our knowledge, OA is the first identified ligand

87   starting from plant crude extracts, as well as the first known strong acidic ligand for

88   insect Grs.

89

90   **Results**

91   **Oxalic acid is a ligand of NlGr23a**

92   To identify the specific ligand of NlGr23a, we cloned the full-length *NlGr23a* open

93   reading frame (GenBank accession No. MT387198), which encodes 451 amino acid

94   residues with seven predicted transmembrane domains (see Appendix 1—figure 1A).

95   Then NlGr23a-expressing stable *Spodoptera frugiperda* (Sf9) cell line was

96   established by antibiotic selection for at least 10 passages. Expression of the stably

97   transfected gene was verified by immunoblotting and RT-PCR (see Appendix

98   1—figures 1B and C).

99   We carried out 4 rounds of ligand screening to search for potential ligands of

100   NlGr23a from crude extracts of rice stems and leaves. The initial calcium imaging

101   results revealed that the ethyl acetate (EAC) and methyl alcohol (MeOH) fractions

102   caused significantly higher calcium ion release/concentration (i.e. cellular response)

103   as indicated by the ratio of cytoplasmic fluorescence intensities (Figure 1A). The

4

104 EAC fraction was then further fractionated into three portions for the next round of

105 screening; Sf9 cells expressing *NlGr23a* showed a response only to fraction 2 (time of

106 retention, $t_R = 20$–35 min, Figure 1B and see also Appendix 1—figure 2A for HPLC

107 chromatogram of the EAC fraction). This fraction was subjected to further

108 fractionation with acetonitrile (ACN) and we found that only the subfraction collected

109 in 5–10 min specifically evoked Ca^{2+} release (Figure 1C and see also Appendix

110 1—figure 2B for HPLC chromatogram of the subfraction). The bioassay-positive

111 subfraction was isolated and analysed using gas chromatography-mass spectrometry

112 (GC-MS). Four compounds, oxalic acid (OA), glycerol, phthalic acid, and trisiloxane,

113 were identified (Figure 1D and see also Appendix 1—figure 2C for GC-MS

114 chromatogram of the control solution). As the peak intensity of phthalic acid was

115 quite weak, and trisiloxane was probably an artefact of culture vessel silanization (see

116 Appendix 1—table 1 for the GC-MS analysis details), OA and glycerol were selected

117 as potential ligands. Tests using commercial OA and glycerol showed that

118 NlGr23a-Sf9 cells responded dramatically to OA stimulation (Figure 1E).

119 In addition, expressing NlGr23a in the human embryonic kidney 293T (HEK293T)

120 cells also allowed these cells to respond to OA. This suggests that NlGr23a showed

121 full functionality in Sf9 cells without an insect-specific co-receptor (Figure 1F). The

122 responses elicited by the HEK293T cells increased with higher acid concentrations

123 and were inversely correlated with pH of OA solution (Figs 1G and H). Microscale

124 thermophoresis assay, which has been used to measure binding affinities, supported

125 the results that NlGr23a interacts with OA. As seen in Figure 1—figure supplement

126 1A, when NlGr23a-GFP was mixed with different concentrations of glycerol, there

127 was no fluorescence migration change after laser irradiation, suggested that the

128 binding state of NlGr23a did not change by glycerol, whereas when NlGr23a-GFP

129 was mixed with different concentrations of OA, the fluorescence migration via laser

130 irradiation gradually decreased as the concentration of OA increases. Thus, OA was

131 shown to be a ligand of NlGr23a. As NlGr23a interacted with bioactive molecules in

132 the MeOH fraction, NlGr23a may also have non-OA ligands in rice (Figure 1A). To

133 characterize the response profiles of NlGr23a, we tested responsiveness of the

5

134   NlGr23a-expressing HEK293T cells to ten additional phytochemicals. Stimulation

135   with only benzoic acid induced a Ca^{2+} increase, whereas stimulation with other

136   organic acids, which have shown inhibitory effects against BPHs, elicited no response

137   (Yoshihara *et al.*, 1980) (Figure 1—figure supplement 1B). No response was also

138   observed in sucrose, various bitter compounds and HCl (Figure 1—figure supplement

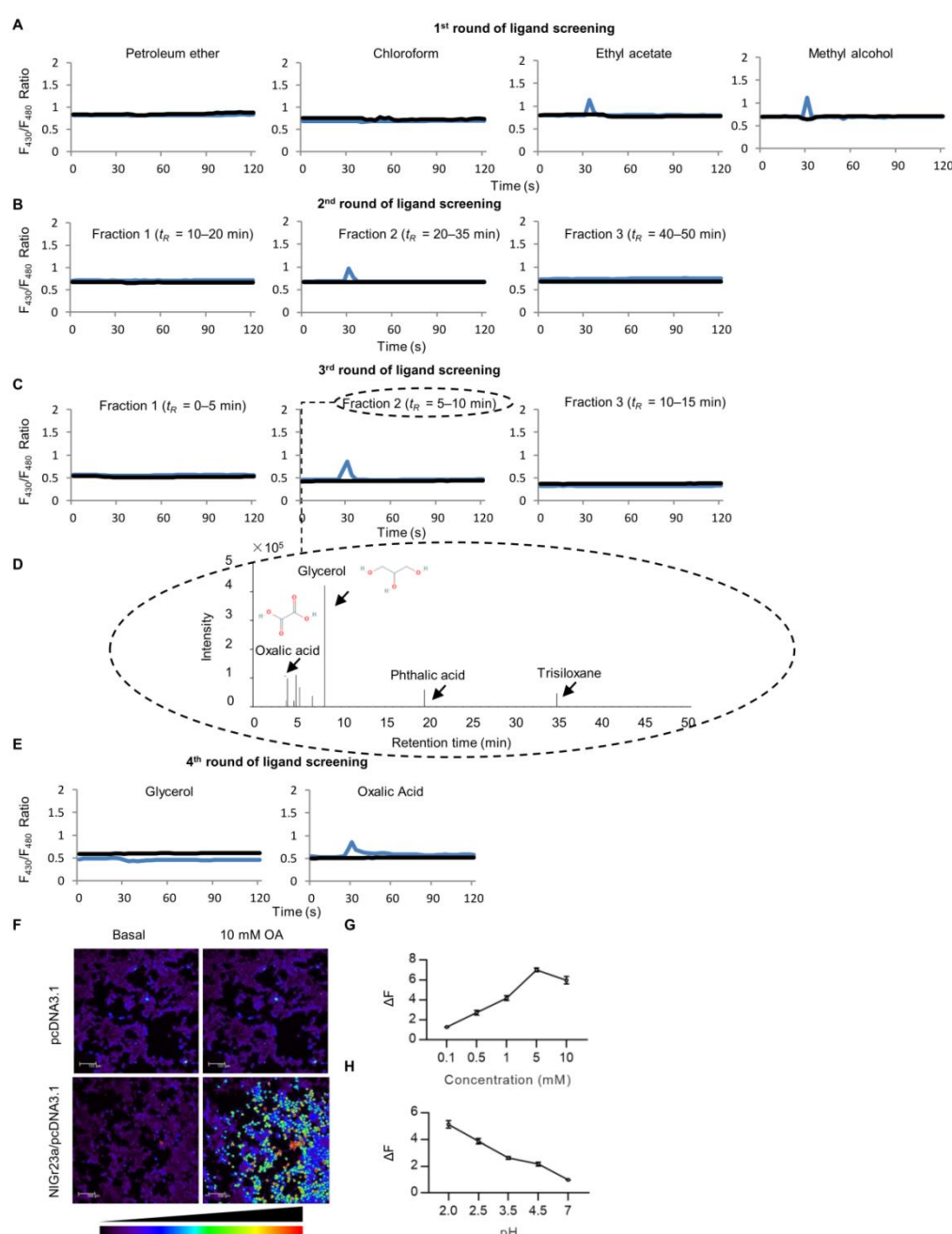139   1B). Hence, NlGr23a may mediate carboxylic acids sensing in a structure dependent

140   manner.

141

142

143 **Figure 1. Oxalic acid is a ligand of NlGr23a.**

144 (A) Round 1 of ligand determination. The responses of Sf9 cells transfected with

145 plasmid construct pIZ-NlGr23a-V5-His (blue lines) or pIZ-V5-His (black lines)

146 vector to different fractions and tastants were analysed by calcium imaging. The

147 changes in intracellular Ca^{2+} indicated by the ratio of F_{340}/F_{380} in Fura-2 AM loaded

148 cells in response to fractions of the crude extract obtained with petroleum ether (PE),

149 chloroform ($CHCl_3$), ethyl acetate (EAC) and methyl alcohol (MeOH) were measured

150 using microscopy. Test solutions are shown above each figure. Each curve represented

151 one cell responding to a specific tastant.

152 (B) Round 2 of ligand determination. Representative traces evoked by three

153 semi-preparative high-performance liquid chromatographic (semi-prep-HPLC)

154 fractions separated from the EAC fraction. See Appendix 1—figure 2A for HPLC

155 chromatogram of the EAC fraction.

156 (C) Round 3 of ligand determination. Representative traces evoked by three

157 semi-prep-HPLC fractions separated from the bioassay-positive fraction from round 2

158 of ligand screening. See Appendix 1—figure 2B for HPLC chromatogram of the

159 bioassay-positive subfraction.

160 (D) GC-MS chromatogram of bioassay-positive fraction from round 3 of ligand

161 screening. Arrowheads indicate substances identified in the bioassay-positive fraction.

162 See Appendix 1—figure 2C for GC-MS chromatogram of the control solution and

163 Appendix 1—table 1 for the retention time and response intensity of each compound.

164 Chemical structure of oxalic acid (OA, PubChem CID: 971) and glycerol (PubChem

165 CID: 753) were obtained from *PubChem* (https://pubchem.ncbi.nlm.nih.gov).

166 (E) Round 4 of ligand determination. Representative traces evoked by 5 mM glycerol

167 and 5 mM OA.

168 (F) Cytoplasmic Ca^{2+} imaging of the HEK293T cells expressing NlGr23a. Upper: the

169 pcDNA3.1 transfected HEK293T cells. Lower: the NlGr23a/pcDNA3.1 transfected

170 HEK293T cells. Left: Fluorescence image before 10 mM OA perfusion. Right:

171 Fluorescence image after 10 mM OA perfusion. White scale bar indicates 100 μm.

172 The color scale indicates the cytoplasmic fluorescence ratio.

7

173   (G) Ca^{2+} response of the NlGr23a-HEK293T cells ($n = 50$) stimulated with various

174   concentrations of OA solutions. ΔF represented the values of F_{340}/F_{380} ratio, which

175   were set to 1 before the addition of the OA solution. Bars represent means $\pm$ SEM.

176   (H) Ca^{2+} response of the NlGr23a-HEK293T cells ($n = 50$, except for pH = 4.5, where

177   n = 27) stimulated with 10 mM OA at different pH. ΔF represented the values of

178   F_{340}/F_{380} ratio, which were set to 1 before the addition of the compound. pH was

179   adjusted using NaOH. Bars represent means $\pm$ SEM.
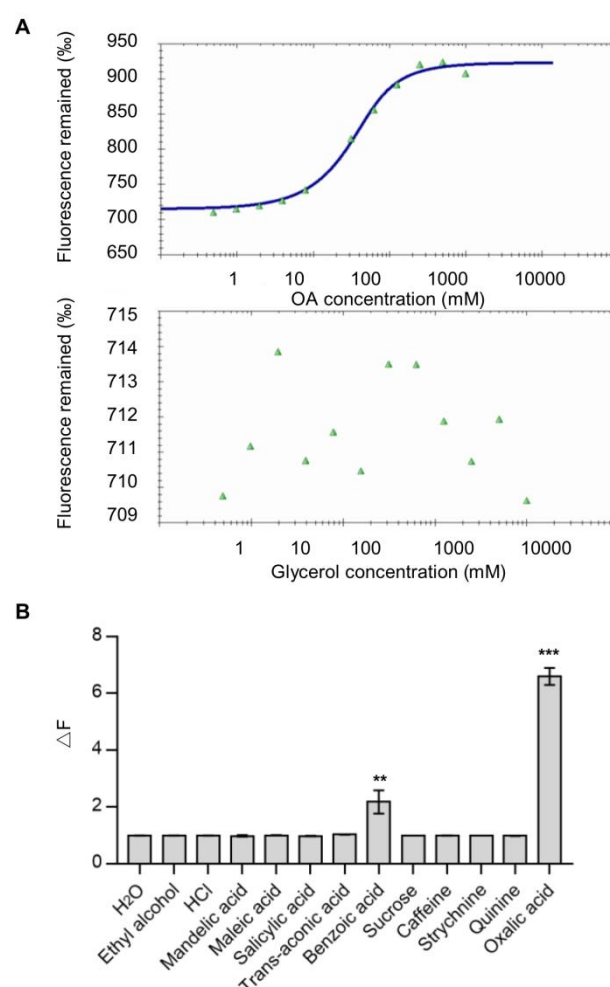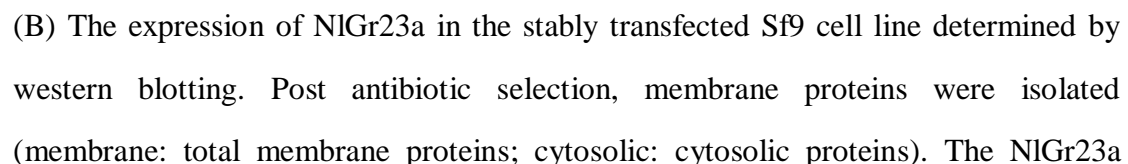
180

181

182   **Figure 1—figure supplement 1. Verification of interaction between NlGr23a and**

183   **oxalic acid (OA) and response profiles of the HEK293T cells expressing NlGr23a.**

184   (A) Verification of interaction between NlGr23a and OA using microscale

185   thermophoresis. Top: The interaction of NlGr23a-GFP with OA. Bottom: The

8

186 interaction of NlGr23a-GFP with glycerol. Sf9 cells transfected with

187 pIZ-NlGr23a-GFP were harvested and lysed 3 days post transfection. The cell lysates

188 were mixed with equal volume of 2 fold gradient diluted OA or glycerol respectively

189 and used for microscale thermophoresis.

190 (B) Responsiveness of the NlGr23a-HEK293T cells to other phytochemicals. Ca^{2+}

191 response of the NlGr23a-expressing HEK293T cells (n = 50) was stimulated with

192 indicated tastants (each at 10 mM). Bars represent means $\pm$ SEM. t-test; $**P < 0.01$;

193 $***P < 0.001$.

194

195 **Appendix 1**

196

197 **Appendix 1—figure 1. The gene structure of *NlGr23a* and NlGr23a expressed in**

198 **Sf9 cells.**

199 (A) Nucleotide and deduced amino acid sequences of *NlGr23a* cDNA. The predicted

200 seven transmembrane domains (TMs) are shaded in grey. "*" represents the terminal

201 codon.

202 (B) The expression of NlGr23a in the stably transfected Sf9 cell line determined by

203 western blotting. Post antibiotic selection, membrane proteins were isolated

204 (membrane: total membrane proteins; cytosolic: cytosolic proteins). The NlGr23a

9

205   expression was detected by the anti-V5 antibody. For membrane proteins visualization,

206   the antibody against β-actin was used as the loading control. Stripping protocol was

207   performed using western blot stripping buffer on the same membrane to obtain

208   β-actin signal. NlGr23a/pIZ-V5-His represents pIZ-NlGr23a-V5-His vector

209   transfected cells. CK represents non-transfected cells and pIZ-V5-His represents

210   pIZ-V5-His vector transfected cells as the negative controls.

211   (C) The expression of *NlGr23a* in the stably transfected Sf9 cell line examined by

212   RT-PCR. Post antibiotic selection, RNA from the transfected Sf9 cells was isolated

213   and subjected to RT-PCR analysis of *NlGr23a* transcription.

214

215
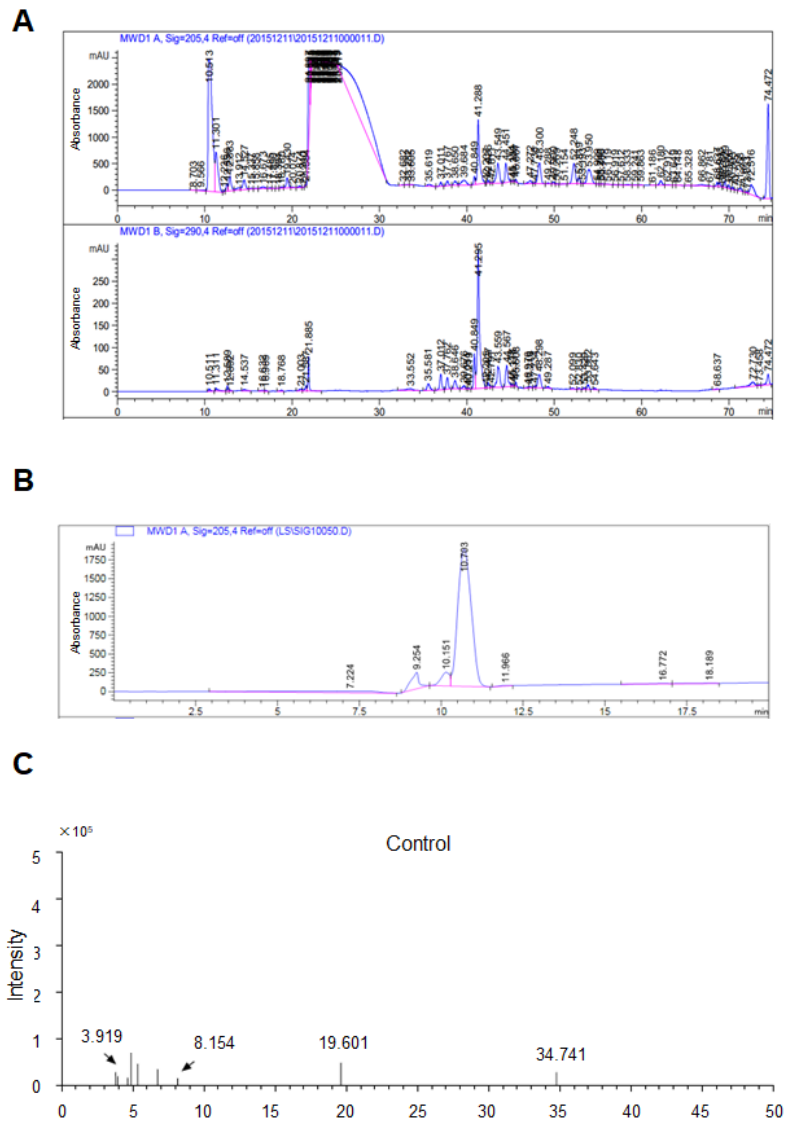
216   **Appendix 1—figure 2. Isolation and identification of rice crude extracts.**

217   (A) HPLC chromatogram of the ethyl acetate fraction. The UV detection wavelengths

218   were set at 205 nm (top) and 290 nm (bottom).

219   (B) HPLC chromatogram of bioassay-positive fraction from round 2 of ligand

220   screening. The UV detection wavelength was set at 205 nm.

221   (C) GC-MS chromatogram of the control solution.

222

Retention time (min)		Intensity		Name
Control	Sample	Control	Sample	
3.919	3.909	22228	100977	Oxalic acid
8.154	8.144	18117	445691	Glycerol
19.601	19.581	51353	62489	Phthalic acid
34.741	34.691	31094	48765	Trisiloxane

223   **Appendix 1—table 1. Identification of differential peaks by GC-MS.**

224

225   *NlGr23a* **is essential to the antifeedant activity of oxalic acid**

226   BPH adults offered artificial diets either containing (+OA) or missing OA (-OA) with

227   no alternative ("no-choice" tests) showed significantly lower acceptance of +OA

228   compared to -OA after 1.5 h exposure (Figure 2A). When offered a choice

229   ("dual-choice"), +OA food was avoided in favour of -OA food, based on insect

230   positioning relative to the food sources (position index, PI = -0.52, Figure 2B). The

231   electrical penetration graph (EPG) technique, which can discriminate between feeding

232   behaviours by producing different waveforms, was used to investigate the effect of

233   OA on BPH feeding behaviour. Three such waveforms occurred sequentially during

234   the process of BPH feeding on liquid diet sacs (LDS): NP (non-penetration), PW

235   (pathway wave), and N4 (artificial diet ingestion) (Figure 2C, top). At 100 μM OA in

236   the diet (+OA), the pre-feeding phases were longer than those of the control (-OA)

237   and the N4 phase was very significantly shorter (Figure 2C, bottom). OA, even at a

238   low concentration, was thus capable of interfering food sucking behaviour. The

239   proportion of time spent feeding fell further as OA concentrations increased, down to

240   only 0.56% at an OA concentration of 10 mM (Figure 2C, bottom).

241   Further, we added two different food dyes into sucrose solutions with or without

242   OA to measure direct feeding. BPHs were given a choice between 2% (w/v) sucrose

243   and 10% sucrose plus different concentrations of OA. Sucrose is a potent sucking

244   stimulant for BPH (Sogawa, 1982). In the absence of OA, the insects showed a

245   preference for the 5-fold higher concentration of sucrose (Figure 2D). However, when

246   the higher concentration of sucrose was contaminated with OA, BPHs avoided the

247   OA-laced food in a dose dependent manner (Figure 2D). A similar experiment was

248   conducted using an equal concentration of sucrose (10%), BPHs showed similar

249   preference for 10% sucrose solutions added with different food dyes without OA and

250   exhibited repulsion to the food when it was mixed with OA (Figure 2—figure

251   supplement 1A). In addition, BPHs consumed significantly less food containing much

252   less concentration of OA (100 μM) compared to the control (Figure 2—figure

253   supplement 1B). These results indicated that the antifeedant activity of OA was dose

254   dependent. To exclude the possibility of olfaction mediated OA sensing, we surgically

255   removed the primary olfactory organs of BPH, the second and third antennal

256   segments (Aljunid and Anderson, 1983). Antennaectomized insects were normal for

257   OA avoidance (Figure 2—figure supplement 1C). Thus, olfactory system is not

258   required for OA avoidance.

259   As OA was a ligand of the NlGr23a receptor, we hypothesised that the antifeedant

260   activity of OA is dependent on this receptor. The *NlGr23a* gene was therefore silenced

261   using RNA interference (RNAi) *in vivo*. *NlGr23a* expression in the whole insect was

262   decreased significantly 24 to 72 h post-injection (Figure 2—figure supplement 2A).

263   Additionally, *NlGr23a* mRNA levels in primary gustatory organs at 48 h post

264   injection substantially decreased compared to the negative controls (Figure 2—figure

265   supplement 2B). As the tissue amount of tarsus was insufficient for RNA extraction,

266   we extracted RNA from legs to detect the gene silencing efficiency. As expected, the

267   antifeedant activity of OA was decreased in *NlGr23a*-inactive insects compared to the

268   control insects injected with green fluorescent protein (*GFP*) double-stranded RNA

269   (dsRNA) in no-choice tests. In BPHs fed -OA artificial diets, the level of food

270   acceptance was nearly the same for both treated (ds*NlGr23a*) and control (ds*GFP*)

groups (Figure 2E, top). In insects fed +OA diets, those with silenced *NlGr23a* spent more time on the OA-containing food than controls, significantly so between 1.5 h and 2.5 h after exposure (Figure 2E, bottom). In the dual-choice assays, a decrease in OA's antifeedant effectiveness was also observed. BPHs injected with ds*NlGr23a* were less sensitive to OA (PI=-0.28) than controls (PI=-0.48, Figure 2F). When BPHs fed on diets without OA, the NP duration was higher and the N4 duration was commensurately lower in *NlGr23a*-silenced insects (Figure 2G, left), which indicated that RNAi against *NlGr23a* influenced their feeding behaviour. At 10 mM OA, *NlGr23a*-silenced BPHs exhibited significantly more N4 and PW phases and fewer NP phases than controls (Figure 2G, right). Similar results were observed at 2 mM or 5 mM OA (Figure 2—figure supplement 2C). Additionally, knockdown of *NlGr23a* dramatically reduced OA feeding avoidance (Figure 2H). Taken together, these results indicated that *NlGr23a*-silenced BPHs were less sensitive to OA.
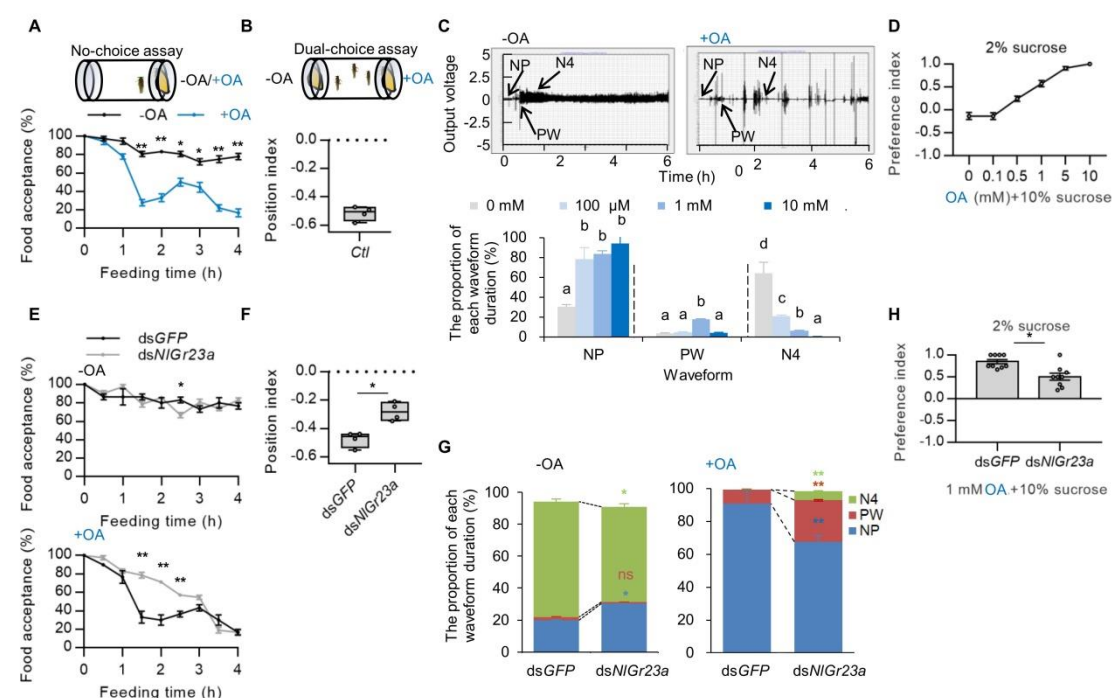

Figure 2. Effects of *NlGr23a* on the antifeedant activity of oxalic acid.

(A) Top: Schematic representation of the experimental apparatus used for no-choice test. Bottom: The proportion of BPHs accepting artificial diets without (-OA, in black)

289   or with 100 μM OA (+OA, in blue) as food in no-choice test. The data represent

290   means ± SEM. *t*-test; *$P < 0.05$; **$P < 0.01$ ($n = 3$).

291   (B) Top: Schematic representation of the experimental apparatus used for dual-choice

292   test. Bottom: Collective data ($n = 4$) of the position index (PI) of the laboratory

293   insects (*Ctl*) in response to food containing 100 μM OA in dual-choice assays.

294   (C) Top: Overall typical view of electrical penetration graph (EPG) waveforms

295   generated by the feeding behaviours of BPH on liquid diet sacs (LDS) without (top)

296   or with (bottom) 100 μM OA. There are three typical waveforms: non-penetration

297   (NP), pathway (PW), and ingestion (N4). Bottom: The duration of each EPG

298   waveform as a proportion of observation time produced by BPHs on LDS containing

299   artificial diets with different concentrations of OA. Bars represent means + SEM.

300   Different lowercase letters above columns represent significant differences at $P < 0.05$

301   from Duncan's multiple range test ($n = 5$).

302   (D) Dose-responsive food choice assay for OA. BPHs were given the choice between

303   2% sucrose solution and 10% sucrose with different concentrations of OA. The data

304   represent means ± SEM (n = 8).

305   (E) Top: The proportion of insects accepting artificial food in absent of OA (-OA)

306   among ds*GFP*-treated (black line) or ds*NlGr23a*-treated (grey line) BPHs in

307   no-choice tests. Bottom: The proportion of insects accepting artificial food with 100

308   μM OA (+OA) among ds*GFP*-treated or ds*NlGr23a*-treated BPHs in no-choice tests.

309   The data represent means ± SEM. *t*-test; *$P < 0.05$; **$P < 0.01$ ($n = 3$).

310   (F) PI values of ds*NlGr23a*-treated and ds*GFP*-treated BPHs in response to +OA diets

311   in dual-choice assays. *t*-test; *$P < 0.05$ ($n = 4$).

312   (G) The duration of each EPG waveform as a proportion of observation time

313   produced by ds*GFP*-treated and ds*NlGr23a*-treated BPHs on LDS with or without 10

314   mM OA. Stacked bar graphs represent means + SEM. *t*-test; ns, $P > 0.05$; *$P < 0.05$;

315   **$P < 0.01$ ($n = 5$).

316   (H) Food choice assay for ds*NlGr23a*-treated and ds*GFP*-treated BPHs. 1 mM OA

317   was mixed with 10% sucrose. Bars represent means ± SEM. *t*-test; *$P < 0.05$ (n ≥ 7).
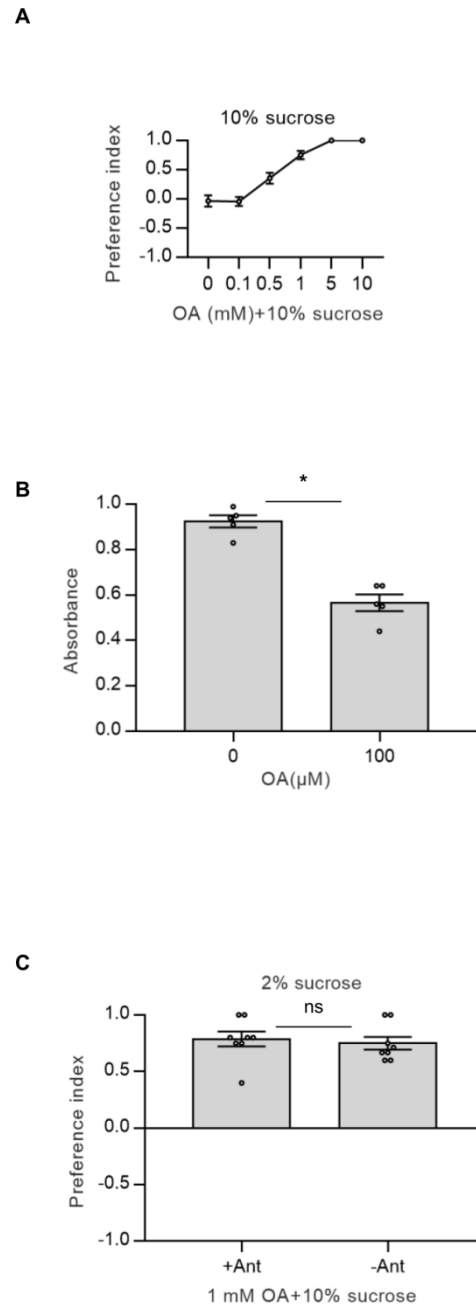
318

A

B

C

319

Figure 2—figure supplement 1. OA induced feeding avoidance.

(A) Dose-responsive food choice assay for OA using an equal concentration of sucrose. BPHs were given the choice between 10% sucrose solution and 10% sucrose with different concentrations of OA. The data represent means $\pm$ SEM. (n$\geqslant$8).

(B) Effect of OA on food ingestion. Amount of ingestion was calculated using spectrophotogram analysis for diets with or without 100 μM OA. Bars represent means $\pm$ SEM. t-test; *$P < 0.05$ (n = 5).

15

327   (C) Role of olfaction in OA avoidance. Bars represent means $\pm$ SEM. t-test; ns, $P >$
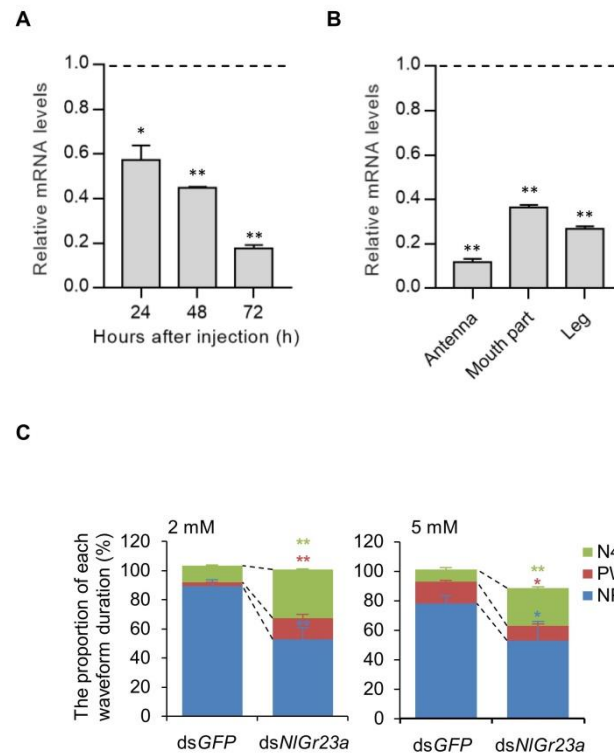
328   0.05 (n=8).

329

330

331   **Figure 2—figure supplement 2. Electrical penetration graph results for BPHs**

332   **feeding on liquid diet sacs (LDS) after *NlGr23a* silencing and OA content in**

333   **different rice varieties.**

334   (A) The messenger RNA (mRNA) levels of *NlGr23a* in BPH 24, 48 and 72 h after

335   injection of *NlGr23a* dsRNA. All mRNA levels were normalized relative to the

336   *β*-actin mRNA levels. The mRNA level of *GFP* was set to 1. Bars represent means +

337   SEM. t-test; $*P < 0.05$; $**P < 0.01$ (n = 3).

338   (B) The mRNA levels of *NlGr23a* in primary gustatory organs at 48 h post injection

339   of *NlGr23a* dsRNA. All mRNA levels were normalized relative to the *β*-actin mRNA

340   levels. The mRNA level of *GFP* was set to 1. Bars represent means + SEM. t-test;

341    $**P < 0.01$ (n =3).

342   (C) The duration of each waveform as a proportion of observation time produced by

343   ds*NlGr23a*- and ds*GFP*- treated BPHs on LDS containing artificial diets with 2 mM

16

344   or 5 mM OA. Stacked bar graphs represent means + SEM. *t*-test; *$P < 0.05$; **$P <$

345   0.01 (n = 5).

346

347   **Appendix 2**

Primer name	Sequence (5'-3')
NlGr23a-ORF-F	ATGCTGAAAAATAAAAGGTTGCAATC
NlGr23a-ORF-R	CTCGAGAGACTGATATTGCTGTT
NlGr23a-HindIII-F	CCCAAGCTTATGCTGAAAAATAAAAGGTTGCAATC
NlGr23a-EcoRI-R	CGGAATTCCCTCGAGAGACTGATATTGCTGTT
NlGr23a-dsRNA-F	TTACCATTTTTGGACTGGACTA
NlGr23a-dsRNA-R	ACTGCAGTTAAAGTTGATATT
T7-*NlGr23a*-dsRNA-F	GGATCCTAATACGACTCACTATAGGTTACCATTTTTGGACTGGACTA
T7-*NlGr23a*-dsRNA-R	GGATCCTAATACGACTCACTATAGGACTGCAGTTAAAGTTGATATT
NlGr2-dsRNA-F	CACTTCATCTACTTGATGTCCG
NlGr2-dsRNA-R	ATCTCTTATTTCTGCTTGTTTC
T7-*NlGr2*-dsRNA-F	GGATCCTAATACGACTCACTATAGGCACTTCATCTACTTGATGTCCG
T7-*NlGr2*-dsRNA-R	GGATCCTAATACGACTCACTATAGGATCTCTTATTTCTGCTTGTTTC
NlGr11-dsRNA-F	CGCAGACTTGAACAAAGGACCG
NlGr11-dsRNA-R	GTGGTCCATAGATGCGTATAAT
T7-*NlGr11*-dsRNA-F	GGATCCTAATACGACTCACTATAGGCGCAGACTTGAACAAAGGACCG
T7-*NlGr11*-dsRNA-R	GGATCCTAATACGACTCACTATAGGGTGGTCCATAGATGCGTATAAT
NlGr13-dsRNA-F	TTTTTGAGATTCGGAAGAATGT
NlGr13-dsRNA-R	AGTGTGGTATGGTGTCGAGGGA
T7-*NlGr13*-dsRNA-F	GGATCCTAATACGACTCACTATAGGTTTTTGAGATTCGGAAGAATGT
T7-*NlGr13*-dsRNA-R	GGATCCTAATACGACTCACTATAGGAGTGTGGTATGGTGTCGAGGGA
NlGr15-dsRNA-F	TTCCCAAAAACACCAAGC
NlGr15-dsRNA-R	TCAATTTCCTCACAGCCA
T7-*NlGr15*-dsRNA-F	GGATCCTAATACGACTCACTATAGGTTCCCAAAAACACCAAGC
T7-*NlGr15*-dsRNA-R	GGATCCTAATACGACTCACTATAGGTCAATTTCCTCACAGCCA
NlGr17-dsRNA-F	GAAGGGCTACACCTGCACTT
NlGr17-dsRNA-R	GCAGAACAACACCGACACAC

Primer name	Sequence (5'-3')
T7-*NlGr17*-dsRNA-F	GGATCCTAATACGACTCACTATAGGGAAGGGCTACACCTGCACTT
T7-*NlGr17*-dsRNA-R	GGATCCTAATACGACTCACTATAGGGCAGAACAACACCGACACAC
NlGr18-dsRNA-F	GGAAAATATTGTGTTACTGG
NlGr18-dsRNA-R	ATTGATACCACATCGCTGAT
T7-*NlGr18*-dsRNA-F	GGATCCTAATACGACTCACTATAGGGGAAAATATTGTGTTA CTGG
T7-*NlGr18*-dsRNA-R	GGATCCTAATACGACTCACTATAGGATTGATACCACATCGCTGAT
NlGr21-dsRNA-F	TTTGTCATTGTTGAAGGGCTAC
NlGr21-dsRNA-R	ATACTTTGAGATTTGAGGTGGG
T7-*NlGr21*-dsRNA-F	GGATCCTAATACGACTCACTATAGGTTTGTCATTGTTGAAGGGCTAC
T7-*NlGr21*-dsRNA-R	GGATCCTAATACGACTCACTATAGGATACTTTGAGATTTGAGGTGGG
NlGr26-dsRNA-F	ATGAGGGAAGGAGACGAAA
NlGr26-dsRNA-R	TAGGAAGAAGTGAAAGCGC
T7-*NlGr26*-dsRNA-F	GGATCCTAATACGACTCACTATAGGATACTTTGAGATTTGAGGTGGG
T7-*NlGr26*-dsRNA-R	GGATCCTAATACGACTCACTATAGGTAGGAAGAAGTGAAAGCGC
Q-*β*-actin-F	TGCGTGACATCAAGGAGAAGC
Q-*β*-actin-R	CCATACCCAAGAAGGAAGGCT
Q-*NlGr23a*-F	TAGGCAAGAAGTTTGTGGACAG
Q-*NlGr23a*-R	ATGAGATAAGTGAGACACCCGG
Q-*NlGr2*-F	GACCTCCACCTAGTGTCCTG
Q-*NlGr2*-R	TCTGTAGCTGGGCCAACTTT
Q-*NlGr11*-F	TGTCTTGCCTCACCAAACGC
Q-*NlGr11*-R	GCAGCACCAGGTAGCCGAAT
Q-*NlGr13*-F	GCAGCCCTTATTCTTGAGCT
Q-*NlGr13*-R	ACAAGGCTGGCTAGAATGAATG
Q-*NlGr15*-F	TCACCGGAGCAAGTCTTCAT
Q-*NlGr15*-R	CCACATCCAAAACCCGTCTC
Q-*NlGr17*-F	CCCTGCCCAGATTTCGTTAC
Q-*NlGr17*-R	CGTGAGGAATATGAGCAGCG
Q-*NlGr18*-F	TTGTGGTTCTACGTGCGTTG
Q-*NlGr18*-R	ACCCAGATATTCCTCGCTTCA
Q-*NlGr21*-F	CTGTTTCTCTCCTCGCTCGA
Q-*NlGr21*-R	GATTCTGGCTCTCTTTGGCG
Q-*NlGr26*-F	GAGGTGCTTCATCAGAGGGA
Q-*NlGr26*-R	GACGATCTTGACAAGGCTGC

348   **Appendix 2—table 1. Primers used in this study.**

349

350   *NlGr23a* **is required for perception of oxalic acid in rice**

351   To further verify above results in rice plants, we used the immersion method to

352   increase the OA content of the rice variety TN1, resulting in 40% higher content in the

353   OA-treated rice plants (TN1^{+OA}) than in the untreated controls (Figure 3A). Insects

354   fed TN1^{+OA} showed a positional avoidance response (PI =-0.24) and made twice as

355   many probing marks (caused by insects testing food for palatability and withdrawing)

356   as those fed TN1, indicating that BPHs spent more time searching for food on TN1^{+OA}

357   (Figs 3B and 3D). There were also three main types of EPG waveforms occurred

358   during the process of BPH feeding on a rice stem: NP (non-penetration), PW

359   (pathway wave) and N4 (phloem ingestion). Compared to the control group reared on

360   TN1, BPHs fed TN1^{+OA} exhibited longer PW and shorter N4 durations, and thus less

361   phloem ingestion (Figure 3F). Our analysis therefore indicated that BPH feeding was

362   inhibited as the content of OA in rice plants increased.

363   The positional avoidance response disappeared in ds*NlGr23a*-treated BPHs (PI =

364   0.01) but not in ds*GFP*-treated insects (PI = -0.22) (Figure 3C). In addition,

365   ds*GFP*-treated BPHs produced 77% more probing marks on TN1^{+OA} rice plants than

366   on TN1, but this difference also disappeared after injection of *NlGr23a* dsRNA

367   (Figure 3E). EPG results further supported this phenomenon. The proportion of time

368   in the N4 waveform was significantly lower and PW waveform was significantly

369   higher when BPHs fed on TN1^{+OA} in ds*GFP*-treated group, but this significant

370   difference no longer existed after *NlGr23a* was silenced (Figure 3G). These results

371   further confirmed that *NlGr23a* mediated OA perception in rice.

372   As we observed, the PI values in dual choice tests in rice tended to be higher than

373   those from tests using the artificial diet containing OA (Figs 2B and 3B). There are

374   three explanations. Firstly, in the case of the artificial diets, the diets either included or

375   completely excluded OA, while in the case of rice plants, the OA content in TN1^{+OA}

376   was only 39% higher than in TN1 (Figure 3A). Secondly, BPHs tend to move up and

377   down along the same plant instead of quickly moving to a different plant. Thirdly, rice

378   plants contain many metabolites including both deterrents and stimulants to feeding

379   (Yoshihara *et al.*, 1980; Zhang *et al.*, 1999).
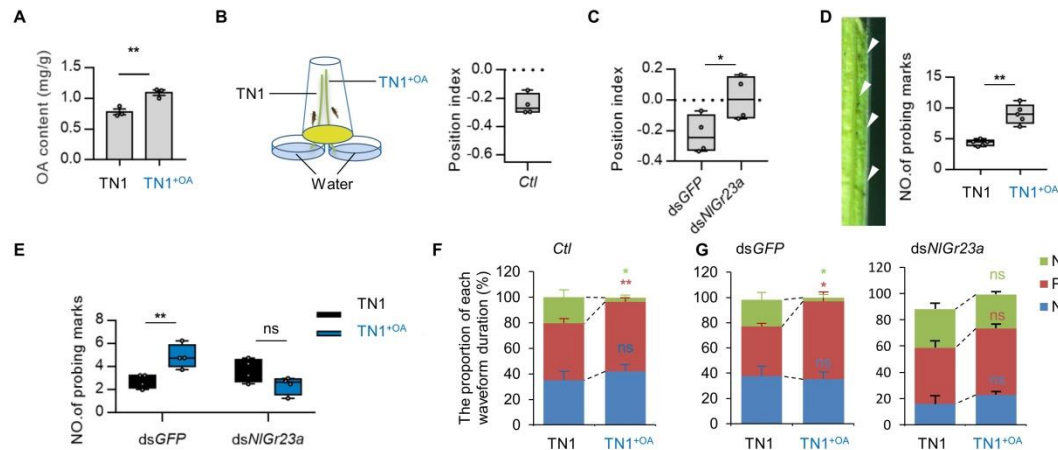
380

381

382   **Figure 3. Increased OA content in rice plant inhibited feeding behaviour of BPH.**

383   (A) OA content before and after immersion treatment in TN1. The TN1^{+OA}

384   represented TN1 treated with 0.2% OA solution. Bars represent means $\pm$ SEM. *t*-test;

385   **$P < 0.01$ ($n = 4$).

386   (B) Left: Schematic representation of the experimental apparatus used for dual-choice

387   test with rice plants. Right: Collective data ($n = 4$) of the position index (PI) of *Ctl* in

388   response to TN1^{+OA}.

389   (C) PI values for *NlGr23a* dsRNA-treated and *GFP* dsRNA-treated BPHs in response

390   to TN1^{+OA} in dual choice assays. *t*-test; *$P < 0.05$ ($n = 4$).

391   (D) Left: Probing marks left on the surface of a rice stem. Right: Collective data ($n =$

392   5) of the number of probing marks on the surface of TN1^{+OA} or TN1 after BPH

393   infestation. *t*-test; **$P < 0.01$.

394   (E) Collective data ($n = 4$) of the number of probing marks on the surface of TN1^{+OA}

395   or TN1 made by BPHs treated with *NlGr23a* dsRNA or *GFP* dsRNA. *t*-test; ns, $P >$

396   0.05; **$P < 0.01$.

397   (F) The duration of each EPG waveform as a proportion of observation time produced

398   by BPHs on TN1 or TN1^{+OA}. Stacked bar graphs represent means + SEM. *t*-test; ns,

399    $P > 0.05$; *$P < 0.05$; **$P < 0.01$ ($n = 5$).

20

400   (G) The duration of each waveform as a proportion of observation time produced by

401   *NlGr23a*-silenced and *GFP* dsRNA-treated BPHs on TN1 or TN1^{+OA}. Bars represent

402   means + SEM. *t*-test; ns, *P* > 0.05; *P <0.05.

403

NlGr23a is also indispensable for sensing OA via BPH tarsi

405   Given that *NlGR23a* was highly expressed in the tarsus (Figure 4A), we developed a

406   novel experiment referred to a previous method (Lee *et al.*, 2010), tarsal avoidance

407   response (TAR) assay, to explore whether *NlGr23a* functioned in OA detection

408   via the tarsi（see Material and Method for the detail of TAR assay). We first

409   determined the behavioral significance of OA to the tarsal behavior by presenting

410   sucrose or sucrose plus OA as a stimulus to the legs. The tarsi preferably adhere to

411   Kimwipe dipped in sucrose (Figure 4B and see also Figure 4—video supplement 1).

412   However, the tarsi elicited TAR after adding OA into sucrose solution (Figure 4B and

413   see also Figure 4—video supplement 2). A small increase was observed in TAR in the

414   second exposure of sucrose alone, likely due to the residual OA effects. Moreover, we

415   observed that OA solution triggered a TAR in a dose dependent manner (Figure 4C).

416   This experiment clearly indicates that female BPH is equipped with a sensitive

417   detection system for OA in the tarsi. As expected, ds*NlGr23a*-injected BPH exhibited

418   a significant reduction in TAR compare to the control (Figure 4D), which supported

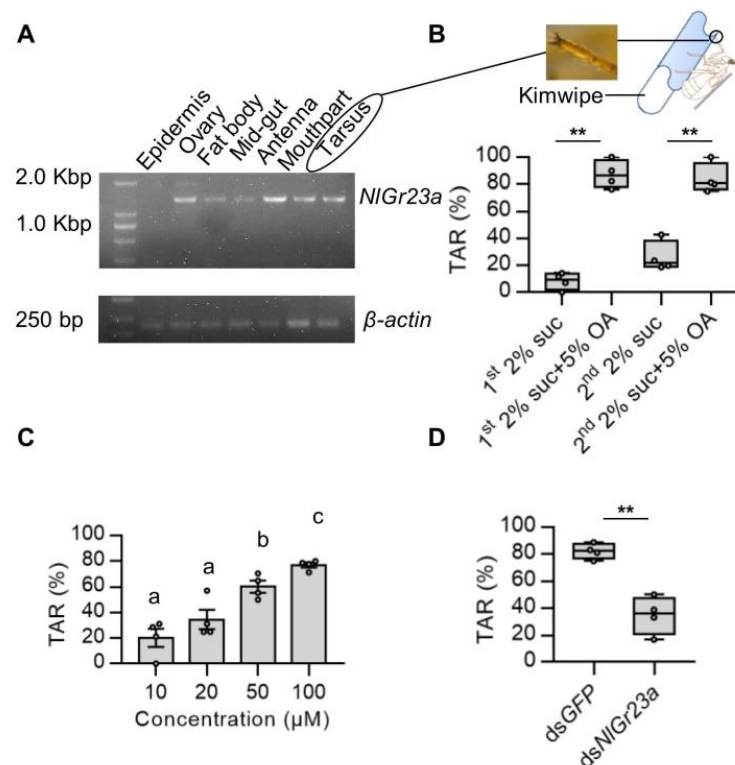419   the idea that *NlGr23a* is indispensable for sensing OA via BPH tarsi.

420

Figure 4. *NlGr23a* is indispensable for sensing OA via BPH tarsi.

(A) RT–PCR of *NlGr23a* on RNA isolated from various organs and tissues. All samples were isolated from one-day-old brachypterous female adults.

(B) Top: Schematic illustration of tarsal avoidance response (TAR) assay for BPHs. Bottom: Collective data ($n = 4$) of TAR of BPHs in response to different stimulants. Insects were initially given 2% sucrose, then 2% sucrose in combination with 5% OA. The trial was conducted two rounds. *t*-test; **$P < 0.01$.

(C) TAR in BPH upon legs stimulation by 10, 20, 50, 100 μM solutions of OA. Bars represent means ± SEM. Different lowercase letters above columns represent significant differences at $P < 0.05$ from Duncan's multiple range test ($n = 4$).

(D) TAR values for *NlGr23a* dsRNA-treated and *GFP* dsRNA-treated BPHs in response to 100 μM OA. *t*-test; **$P < 0.01$ ($n = 4$).

Figure 4—video supplement 1.Tarsal avoidance response (TAR) to sucrose. A Kimwipe containing 2% sucrose was applied to the distal part of legs of BPH. BPH showed acceptance towards the wet wick and its tarsi preferably adhere to Kimwipe.

437

438 **Figure 4—video supplement 2. Tarsal avoidance response (TAR) to oxalic acid.** A

439 Kimwipe containing 2% sucrose plus 5% oxalic acid was applied to the distal part of

440 legs of BPH (the same as the one in Figure 4—video supplement 1) at 5 min interval

441 after 2% sucrose treatment. BPH refused to adhere to the wick and used leg to push

442 away Kimwipe. The hindlegs of BPH did not contact Kimwipe.

443

444 **Discussion**

445 Although insect bitter Grs are assumed to detect plant secondary compounds or bitter

446 tastants (Robertson and Wanner, 2006), it is still very difficult to identify the ligands

447 of bitter Grs, especially new examples. The pioneering identifications typically used

448 electrophysiological and behavioural genetic analyses in Gr mutants of the model

449 insect *D. melanogaster*. Additionally, nearly all of the ligands tested to date have been

450 directly purchased compounds such as caffeine, strychnine, umbelliferone, saponin,

451 chloroquine, and L-canavanine (Moon *et al.*, 2006; Poudel *et al.*, 2015; Shim *et al.*,

452 2015; Poudel *et al.*, 2017; Sang *et al.*, 2019). In other species, especially in

453 agricultural insect pests, Gr ligands are often assumed to match those of the

454 orthologous fruit fly receptors. As non-sugar *Gr* genes are subject to rapid adaptation

455 driven by the vastly different ecological niches occupied by insect species and shared

456 sequence identity among species is low, it is difficult to identify matching receptors.

457 Alternatively, candidate ligands have been chosen from chemical classes that are

458 known to elicit neurophysiological or behavioural responses. For example, a

459 collection of known oviposition stimulants of *Papilionidae xuthus* were selected to

460 test for interaction with PxutGr1, and eventually synephrine was identified as the

461 specific ligand (Ozaki *et al.*, 2011).

462 In order to expand potential ligand sources for non-sugar Grs, plant extracts have

463 been tested in few cases. Extracts of whole citrus caused an increase in

464 Ca^{2+}-dependent luminescence in Sf9 cells after the introduction of *PxutGr1* (Ozaki *et*

465 *al.*, 2011), and similar results were observed for crude extracts of cotton leaves and 3

466 *Grs* in *Helicoverpa armigera* (*HarmGr35*, *HarmGr50*, and *HarmGr195*) (Xu *et al.*,

23

467 2016). However, no specific ligand has so far been identified based on separation of

468 these crude extracts. In this study, we started from rice crude extracts and eventually

469 identified OA as a ligand of NlGr23a. To our knowledge, OA is the first identified

470 ligand starting from plant crude extracts, and the first strong acidic ligand for insect

471 Gr proteins.

472 Grs in insects are known to form heterodimers with co-receptors to recognize the

473 tastant (Dahanukar *et al*., 2007; Lee *et al*., 2009). Nevertheless, there are several

474 instances of the expression of a single insect Gr in a heterologous expression system

475 sufficient to confer tastant responses, including Gr5a, Gr43a and Gr64e from

476 *Drosophila*, BmGr8 and BmGr9 from the silkworm *Bombyx mori*, PxutGr1 from the

477 swallowtail butterfly *Papilio xuthus*, HarmGR35, HarmGR50 and HarmGR195 from

478 the polyphagous pest *Helicoverpa armigera*, AgGr25 from the malaria mosquito

479 *Anopheles gambiae* (Chyb *et al*., 2003; Freeman *et al*., 2014; Sato *et al*, 2011; Zhang

480 *et al*., 2011; Ozaki *et al*., 2011; Xu *et al*., 2016), and PrapGr28 from the cabbage

481 butterfly *Pieris rapae* (Yang *et al*., 2021). In this study, the HEK293T cells expressing

482 NlGr23a caused responses to OA (Figure 1F). But we do not exclude a possibility that

483 NlGr23a requires co-receptors for its fully functionality *in vivo*. Based on the analysis

484 tuned to a 7TMPs characteristic of insect Grs and a homology search with known

485 broadly required gustatory co-receptors, NlGr2, NlGr11, NlGr13, NlGr15, NlGr17,

486 NlGr18, NlGr21 and NlGr26 were selected for food preference assay with 1 mM OA

487 (Kang *et al*., 2018). Gene silencing of the target genes was achieved by dsRNA

488 injection (See Appendix 3—figure 1A for the silencing efficiency of target genes and

489 Appendix 2—table 1 for primers used for dsRNA synthesis and RNAi efficiency

490 detection). Those BPHs treated with ds*NlGr2* and ds*NlGr13* were less sensitive to OA

491 than controls (Appendix 3—figure 1B). These results suggest that NlGr2 and NlGr13

492 might act as co-receptors of NlGr23a for OA recognition or through

493 NlGr23a-independent mechanisms.

494
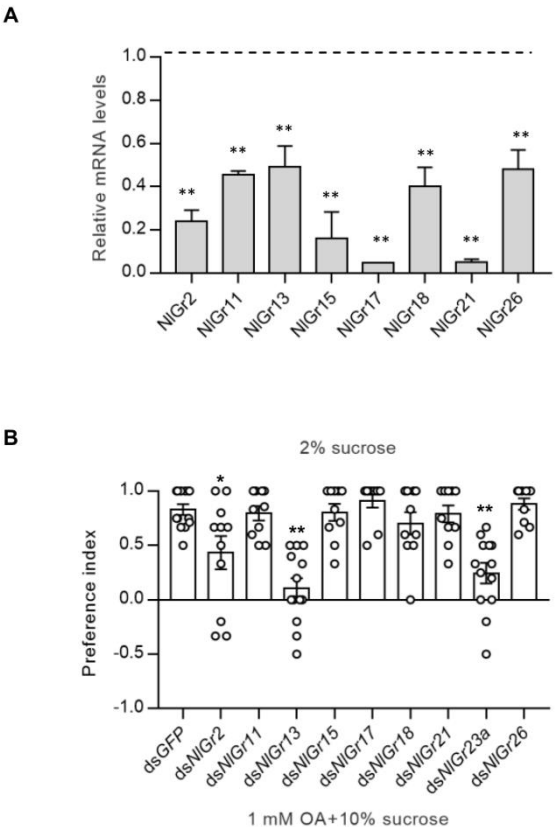
495 **Appendix 3**

Appendix 3—figure 1. Screen of potential co-receptors of NlGr23a using food choice assays.

(A) The mRNA levels of target genes at 48 h post injection of dsRNA. All mRNA levels were normalized relative to the β-actin mRNA levels. The mRNA level of *GFP* was set to 1. Bars represent means + SEM. *t*-test; **$P < 0.01$ (n =3).

(B) Unbiased screen of 8 potential co-recepetors of NlGr23a in binary food choice assays. The data represent means ± SEM. (n≥10). *t*-test; *$P < 0.05$; **$P < 0.01$

OA is, however, commonly present in rice plants. The species of only 11 out of 93 orders of higher plants do not store OA (Zindler-Frank, 1976). The fact that a secondary compound is deterrent to an insect does not imply that the insect does not eat plants containing that compound. Whether or not it does so depends on its sensitivity to the compound, the background of other deterrent and phagostimulatory information in which it is perceived, and the degree of food deprivation incurred by the insect (Chapman, 2003). In the EPG experiments of this study, OA concentrations

25

512 in artificial diets and in rice plants significantly inhibiting feeding phases were 1 mM

513 and about 10 mM (the OA content of the background material TN1 was measured as

514 above 5 mM), respectively (Fig.2C, Fig. 3A and F). The difference in active OA

515 concentration may be due to the different background of other chemicals. Moreover,

516 OA concentrations in rice plants are dynamic, maybe varied in tissues, and affected by

517 rhythm, rice variety and developmental stages, as well as abiotic factors (Wu *et al.*,

518 2016). OA isolated from leaf sheath extracts of rice seems to mediate the

519 phloem-feeding habit as a general inhibitor which commonly occurs in plant tissues

520 outside the phloem (Yoshihara *et al.*, 1980). We also measured OA contents in three

521 rice varieties and indeed found there is a significant difference in OA content between

522 the susceptible TN1 rice and the resistant rice varieties IR36 and IR56 (Appendix

523 4—figure 1). Thus, we speculate that a population of sensory neurons tuned to OA is

524 probably involved in detection of the dynamic changes of soluble OA to provide clues

525 for the suitable habitats or feeding times.

526 **Appendix 4**

527
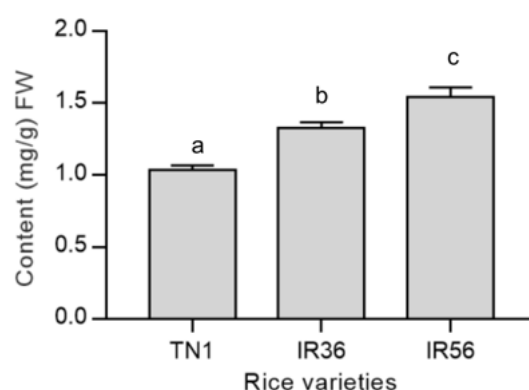
528 **Appendix 4—figure 1. OA content in different rice varieties.** OA content in

529 different rice varieties analysed by HPLC. Bars represent means + SEM. Different

530 lowercase letters above columns represent significant differences at *P* < 0.05 from

531 Duncan's multiple range test (n=4).

532

533   Insects discriminate a wide range of tastants, including sugars, bitter compounds,

534 NaCl, and sour substances. In contrast to sweet and bitter-tasting chemicals, acids

535 elicit varied behavioural responses, depending on their structure and concentration

536 (Rimal *et al.*, 2019). In *Drosophila*, both Ir25a and Gr64a-f expressed in sweet taste

537 neurons mediated appetitive responses to lactic acid (Stanley *et al*., 2021).

538 Knock-down of *Ir25a*, *Ir76b* and *Ir56d* abolished fatty acid recognition (Ahn *et al*.,

539 2017). By screening individual Gr64 cluster gene mutant flies, Gr64e was also

540 identified as a receptor mediating fatty acid sensing (Kim *et al.*, 2018). Ir7a expressed

541 in bitter GRNs is required for rejecting foods laced with high concentrations of acetic

542 acid (Rimal *et al*., 2019). So far, most chemoreceptors repsond to sour tastes are

543 ionotropic receptors, such as Ir25a and Ir76b (Chen and Dahanukar, 2020). In this

544 study, we investigated an important plant-insect interaction and found that NlGr23a in

545 BPH senses OA in rice.

546 It was reported that behavioural repulsion from acidic stimuli is mediated by two

547 different classes of GRN in the fruit fly: those sensing sugar and bitters (Charlu *et al.*,

548 2013; Devineni *et al.*, 2019). This implies that Grs sensing sour compounds may

549 influence insect behaviour through multiple pathways. After *NlGr23a* was silenced,

550 BPHs with *NlGr23a* dsRNA were used for transcriptome and KEGG pathway

551 analysis of the differentially expressed genes. These analyses showed that NlGr23a

552 may function through diverse signalling pathways, including mTOR, AMPK, insulin,

553 and PI3K-AKT (see Appendix 5—figure 1). The possible molecular mechanisms of

554 NlGr23a in modulating feeding behaviour will be further investigated.

555

556 **Appendix 5**

Appendix 5—figure 1. Statistical analysis of enriched pathways for genes differentially expressed between *NlGr23a* dsRNA and *GFP* dsRNA-treated BPHs.

Materials and Methods

Insect and rice culture

A BPH laboratory strain (*Ctl*) was obtained from Guangdong Academy of Agricultural Sciences (GDAAS, Guangdong, China), and this strain was reared in a continuous laboratory culture on susceptible rice seedlings (variety Huang Hua Zhan). All BPHs were maintained at 26 ± 2 ℃ with 80 ± 10% humidity and a light-dark cycle of L16:D8 h. One-day-old brachypterous female adults were collected for the following bioassays. Plants aged 30–40 days of the susceptible rice variety TN1 were used for the relevant bioassays. Allocation of insects was randomly done to minimize the effects of subjective bias.

28

572

Chemical sources

574 OA, glycerine, adonitol, methoxylamine hydrochloride, *N*-methyl-*N*-(trimethylsilyl)

575 trifluoroacetamide, tetrabutylammonium bisulphate (TBA), KH_2PO_4 and strychnine

576 and caffeine (purity, ≥99%) were purchased from Sigma-Aldrich Company (St.

577 Louis, MO, USA). HPLC grade reagents including petroleum ether (PE), chloroform

578 (CH_3Cl), ethyl acetate (EAC), methyl alcohol (MeOH), acetonitrile (ACN), isopropyl

579 alcohol and pyridine, and analytical grade reagents including sucrose, trans-aconitic

580 acid, benzoic acid, salicylic acid, mandelic acid, quinine and ethyl alcohol were all

581 obtained from Aladdin Reagent (Shanghai, China). Maleic acid was purchased from

582 MedChemExpress (Shanghai, China). Hydrochloric acid (HCl) was provided by the

583 Guangzhou Chemical Reagent (Guangzhou, China).

584

Ligand determination for NlGr23a

NlGr23a cDNA cloning and stable cell line construction

587 Total RNA from BPHs was prepared as previously described (Kang *et al.*, 2018). A

588 PrimeScript^{TM} RT reagent kit with gDNA Eraser (Takara, Kyoto, Japan) was used

589 with 1 μg RNA for first-strand complementary DNA (cDNA) synthesis. A fragment of

590 full-length *NlGr23a* cDNA was amplified using 2×SuperStar PCR Mix with Loading

591 Dye (Genstar, Beijing, China) following the manufacturer's instructions. The cloning

592 primers are listed in Appendix 2—table 1.

593 The *NlGr23a* cDNA was inserted into the Hind III and EcoR I sites of pIZ/V5-His

594 vectors (Invitrogen, Carlsbad, CA, USA) using T4 DNA ligase (NEB, Beijing, China).

595 The NlGr23a-Sf9 stable cell lines were obtained by using a previously described

596 method (Chen *et al.*, 2021). Briefly, Sf9 cells were cultured in Grace's Insect Medium

597 (Gibco, Grand Island, NY, USA) supplemented with 10% foetal bovine serum at

598 27 ℃. Cells were plated into 6-well plates and left to settle for 20 min before being

599 transfected with either 2 μg of the recombinant plasmid pIZ-NlGr23a-V5-His or

600 pIZ-V5-His vector (negative control), and 6 μL Fugene HD transfection reagent

601 (Promega, Madison, WI, USA) in 100 μL per well of Grace's Insect Medium.

602   Forty-eight hours after transfection, cells were cultivated under Zeocin selection. The

603   final concentration of Zeocin to maintain cells was 100 μg/mL. Following antibiotic

604   selection for at least 10 passages, stable cell lines were verified by immunoblotting

605   and RT-PCR. For western blotting analysis, cells were lysed by total membrane

606   proteins extraction buffer A (Invent Biotechnologies, Inc., Eden Prairie, USA). The

607   supernatant of the mixture was further centrifuged. The sediment contains the total

608   membrane proteins while the supernatant contains cytosol proteins. Samples were

609   then immunoblotted with anti-V5 antibody. For RT-qPCR, we extracted total RNA of

610   cells after antibiotic selection for cDNA template synthesis. PCR was performed

611   under the following conditions: 94℃ for 2 min, 35 cycles of 94℃ for 30 s, 55 ℃ for

612   30 s, 72℃ for 90 s, and 72℃ for 5 min. PCR amplification products were run on a 1.2%

613   agarose gel.

614   The HEK293T cells were cultured in Dulbecco's modified Eagle medium (Gibco,

615   California, USA) supplemented with 10% fetal bovine serum in an atmosphere of 5%

616   CO_2 and 95% relative humidity at 37 ℃. To confirm the sufficiency of NIGr23a for

617   OA-mediated response, the HEK293T cells were transiently transfected with

618   NlGr23a/pcDNA3.1-FLAG. NlGr23a/pcDNA3.1-FLAG was constructed by inserting

619   a C-terminally FLAG-tagged human codon-optimized *NlGr23a* ORF into the

620   pcDNA3.1 vector using BamHI and EcoRI sites. The nucleotide sequences of the

621   codon-optimized genes were listed in Appendix 6—figure 1. Each 0.5 μg plasmid was

622   transfected into the HEK293T cells using Lipofectamine 3000 (Invitrogen, Carlsbad,

623   CA, USA), according to the manufacturer's instruction.

624

625   **Appendix 6**

```
   1 ATGCTGAAGAACAAGCGCCTGCAAAGTAACAAGAGAGGTATCGGGAGACTGCTGGATATG
   1  M  L  K  N  K  R  L  Q  S  N  K  R  G  I  G  R  L  L  D  M
  61 AGAAACAACAAAGCCGCCACCAAACGCGTCACCTCCCTGCCTCACATTATACATGTGCTG
  21  R  N  N  K  A  A  T  K  R  V  T  S  L  P  H  I  I  H  V  L
 121 GATGTTAACTATAAGACAGCCTATGATTATCATGAGAAGCTGAGGCACTGTATCTACTTC
  41  D  V  N  Y  K  T  A  Y  D  Y  H  E  K  L  R  H  C  I  Y  F
 181 GAACCTATTCAAATAGTCCTCTTCGTCTGGAGCCTGCTGGGCAGACTGCCAATCAGACGC
  61  E  P  I  Q  I  V  L  F  V  W  S  L  L  G  R  L  P  I  R  R
 241 GACTCTACTGGAGACTATATTGTGCCCATTGTCCTCAGAGTGTACAGTTTCCTCGTTGGA
  81  D  S  T  G  D  Y  I  V  P  I  V  L  R  V  Y  S  F  L  V  G
 301 AGTATCATTGTGGTGATTGGCTCAATCAGCCTGAGGAACCTCGTCAAGTCCCTCCTGAAC
 101  S  I  I  V  V  I  G  S  I  S  L  R  N  L  V  K  S  L  L  N
 361 GGCGAGAGCGTGTACGAAGAGCCCACATCTGTGATTGGAGACTACAACTATACACTCTTT
 121  G  E  S  V  Y  E  E  P  T  S  V  I  G  D  Y  N  Y  T  L  F
 421 TGGATCTGTCAGATCCTCGTGACCACTTATAACATTTCCCTGCCCTTCCTGGACTGGACT
 141  W  I  C  Q  I  L  V  T  T  Y  N  I  S  L  P  F  L  D  W  T
 481 ATCGTGGGCGAGTTCCTCAAGTTTCTCCGCAGCTGGGCTCAGTTCCAGGAGAACTATACC
 161  I  V  G  E  F  L  K  F  L  R  S  W  A  Q  F  Q  E  N  Y  T
 541 CTGGAGAGCCGGAAAGTGCTGAGCATCAAGAGCAAGAACAGAATACGCATCATCTTCTAT
 181  L  E  S  R  K  V  L  S  I  K  S  K  N  R  I  R  I  I  F  Y
 601 ATGACTCTGCTGGTGAACATGACCACCGTCGCCTACCTGAACAATTTCGTGATGAAGAAC
 201  M  T  L  L  V  N  M  T  T  V  A  Y  L  N  N  F  V  M  K  N
 661 GTGGATGTGTTTACCAAGATCAGTACCCTCACTGCAGTCGTGGAACTCGAATCCCGCACT
 221  V  D  V  F  T  K  I  S  T  L  T  A  V  V  E  L  E  S  R  T
 721 GCTTTCTTCTGGCATACCTGTGCTGTCATCAGCGATTGCAGCGAACAACTGTCTATCACC
 241  A  F  F  W  H  T  C  A  V  I  S  D  C  S  E  Q  L  S  I  T
 781 TTTTGCAAGAAAACCCTGGAGTCCAGAGTGAGCAGAGGCGCACAGACACTCGGAGATTAC
 261  F  C  K  K  T  L  E  S  R  V  S  R  G  A  Q  T  L  G  D  Y
 841 AGGCGCCTGTGGCTGCAGCTGACCGACACATTACTACTAGTTTCAGCGATCTCATGAGCTAC
 281  R  R  L  W  L  Q  L  T  D  I  T  T  S  F  S  D  L  M  S  Y
 901 AAGATGACCCATTCAATCTTTGTTAATGTGATTTTCGTTATAGTGACTAGTTATCATCTG
 301  K  M  T  H  S  I  F  V  N  V  I  F  V  I  V  T  S  Y  H  L
 961 GCCCTGTCAGCACTGAGCCGCGGAGTTCGCGGCAGTGCTGGAGACATATACCTCTACTTC
 321  A  L  S  A  L  S  R  G  V  R  G  S  A  G  D  I  Y  L  Y  F
1021 TTCTGTTCCCTCTACACAGCAGCCCACGTGATGCTGGCCTGTGAATCCGGCCACAGACTC
 341  F  C  S  L  Y  T  A  A  H  V  M  L  A  C  E  S  G  H  R  L
1081 GCTCAGAGTCTCGGGAAGAAATTTGTTGATCGGGCCACCAGGCGGAGACTCCAACACCTG
 361  A  Q  S  L  G  K  K  F  V  D  R  A  T  R  R  R  L  Q  H  L
1141 TCATTCGCAGAGCGGAAAGAGTTTTCTGTGTTTATGGGCATCGTGCGCAGGAGGTCACCT
 381  S  F  A  E  R  K  E  F  S  V  F  M  G  I  V  R  R  R  S  P
1201 TCAGTCATCCTCAATGGTTTTCTCACCGTCGATCGCAGTCTGATCGTGCTCTTTGTGAGT
 401  S  V  I  L  N  G  F  L  T  V  D  R  S  L  I  V  L  F  V  S
1261 GGATGTCTCACATACCTGATCATTCTCGTGCAATTCAAAGTGGGCATGAGCGAAACTCAT
 421  G  C  L  T  Y  L  I  I  L  V  Q  F  K  V  G  M  S  E  T  H
1321 AGAGTGCAGAATAGCAATATCTCACTCAGCAGG
 441  R  V  Q  N  S  N  I  S  L  S  R
```

Appendix 6—figure 1. The nucleotide sequences of human codon-optimized *NlGr23a* genes.

Isolation and identification of active compounds in rice

A bioassay-guided approach was adopted to isolate and identify active compounds interacting with NlGr23a from the crude extracts of rice plants. Firstly, we ground stems and leaves of TN1 (5 g), and performed serial solvent extractions on macerated subsamples with 25 mL of isopropanol (IPA) at 75 °C for 15 min, 25 mL CHCl$_3$–IPA (1:2, v/v; 5 h; room temperature), and 25 mL MeOH–CHCl$_3$ (2:1, v/v; overnight; room temperature). Each extract was centrifuged at 2,000 rpm for 15 min to collect the supernatant. The pooled supernatants were then concentrated to dryness in vacuum at 25 °C and re-dissolved in 12 mL CHCl$_3$ to obtain the crude rice extract.

639 Secondly, 6 mL crude extract was subjected to a column chromatography with silica

640 gel, eluting with solvents in the order of increasing polarity (PE - CHCl$_3$ - EAC -

641 MeOH) to yield four fractions. We carried out the first round of ligand screening

642 using these four initial fractions. Thirdly, semi-preparative HPLC separation of the

643 bioassay-active fraction I was performed on an Agilent 1260 HPLC system (Agilent

644 Technologies, Santa Clara, CA, USA) equipped with an Agilent ZRBAX SB-C18

645 column (4.6 mm $\times$ 150 mm, 3.5 μm) by gradient elution with ACN (A) and water (B).

646 The gradient program was as follows: 3 min, 5% B; 22 min, 5–20% B; 15 min, 20-40%

647 B; 15 min, 40–50% B; 8 min, 50–95% B; 12 min, 95-5% B, all at a flow-rate of 1

648 mL/min. The eluate from the column was continuously monitored at 205 and 290 nm

649 after sample loading (5 μL), and the fraction collector was programmed to collect

650 fractions during periods in which most substances were detected (see Appendix

651 1—figure 2A). The second round of screening for the ligand was then carried out with

652 these subfractions. Fourthly, the active semi-prep-HPLC fraction (active fraction II)

653 was subjected to further fractionation with 100% ACN at a flow-rate of 1 mL/min for

654 the third round of screening. Last, the bioassay-positive fraction from this latest round

655 (active fraction III) was derivatized and elucidated using GC-MS. The GC-MS

656 detection for the derived samples was performed on an Agilent 7890A gas

657 chromatograph equipped with an Agilent 5975C VL MSD detector (Agilent

658 Technologies, Santa Clara, CA, USA) as previously described (Kang *et al.*, 2019).

659 **Calcium imaging assay**

660 Calcium imaging using fura-2/AM calcium indicator dye was performed as

661 previously described with some modification (Nelson *et al.*, 2001; Chen *et al.*, 2021).

662 Cells were seeded in a glass bottom cell culture dish (φ20 mm, Nest, Jiangsu, China)

663 at 70% confluency and grown overnight. After being washed in Hanks' balanced salt

664 solution (HBSS, Solarbio, Beijing, China) for three times, cells were incubated for 30

665 min with 2 mL HBSS, which was added with 2μL 1 mg/mL fura-2/AM (Invitrogen,

666 Carlsbad, CA, USA, dissolved in DMSO,) under shaking conditions (60 rpm) at room

667 temperature in dark. Subsequently, fura-2/AM solution was removed and cells were

668 then washed twice with HBSS and were covered with 2 mL of fresh HBSS. Imaging

669 experiments were conducted on a Leica live cell imaging microscope (DMI6000B)

670 equipped with a CCD camera. Cells were stimulated with 340 and 380 nm UV light.

671 A 200 μL test solution was added into the dish using pipette. Data acquisition and

672 analysis were performed by using Leica LAS-AF software (version 2.6.0). The

673 F_{340}/F_{380} ratio was analyzed to measure Ca^{2+}. Cell assays were repeated for at least

674 three times. Sample size of cell assays to achieve adequate power was chosen on the

675 basis of a previous report with similar methods (Sato *et al.*, 2011).

676 **Microscale thermophoresis**

677 In this study, the Microscale Thermophoresis device (Nano Temper Technologies) was

678 used for measurements of binding affinities. Briefly, the recombinant plasmid

679 pIZ-NlGr23a-GFP was constructed using the *NlGr23a* ORF with Kozak consensus

680 sequence at the 5' ends and *GFP* coding sequence at the 3' ends cloned into

681 pIZ-V5-His vector. Subsequently, Sf9 cells were transfected with the

682 pIZ-NlGr23a-GFP plasmid (2 μg per 10^6 cells) using Lipo3000. To achieve higher

683 transfection efficiency, a second transfection was performed in the same batch of Sf9

684 cells at 24 h after the first transfection. Cells were harvested 48 h after the second

685 transfection. After one wash in PBS, cells were lysed in RIPA lysis buffer and then

686 incubated on a rotary table. After samples were rotated for 1.5 h, the lysates were

687 centrifuged at 13,000 xg for 15 min at 4 ℃. The extract was harvested and separated

688 into 5 μL per portion; each portion of cell lysate was mixed gently with equal volume

689 of 2 fold gradient diluted OA or glycerol respectively and used for microscale

690 thermophoresis under procedures described previously (Wienken *et al.*, 2010).

691

692 **RNAi treatments**

693 **dsRNA preparation and injection into BPH**

694 Template DNA for dsRNA synthesis was amplified using gene-specific primers (see

695 see Appendix 2—table 1). The resulting purified products were then used to

696 synthesize dsRNA using a MEGAscript T7 High Yield Transcription Kit (Promega,

697 Madison, WI, USA). The concentration of *NlGr23a* dsRNA (239 bp) was quantified

698 with a NanoDrop 2000 instrument (Thermo Fisher Scientific, Waltham, MA, USA).

33

699   Finally, the quality and size of the dsRNA were further verified via electrophoresis in

700   a 1% agarose gel. *GFP* dsRNA was used as a control. BPHs were collected from the

701   culture chamber and anaesthetized with CO_2 for 20 s. Approximately 250 ng dsRNA

702   was injected into each individual. After injection, the BPHs were reared on fresh rice

703   plants, which were maintained in transparent polycarbonate jars measuring 15 cm in

704   diameter and 70 cm in height. Individuals exhibiting motor dysfunction and/or

705   paralysis in 12 h were excluded for next steps. Total RNA of whole body was

706   extracted from five randomly selected individuals to examine the gene silencing

707   efficiency at different time-points (24 h, 48 h and 72 h) by quantitative reverse

708   transcription PCR (qRT–PCR). Total RNA of antennae, mouthparts and legs

709   separately dissected from 30 females 48 h after ds*NlGr23a* injection was subjected to

710   examine the gene silencing efficiency in primary gustatory organs. Feeding bioassays

711   were conducted 48 h after injection.

712   **qRT-PCR analysis**

713   The qRT-PCR procedure was performed using a Light Cycler 480 (Roche Diagnostics,

714   Basel, Switzerland) with a SYBR®FAST Universal qPCR Kit (KAPA, Woburn, MA,

715   USA), following the manufacturer's instructions. Each reaction mixture included 1 μL

716   of cDNA template equivalent to 1 ng of total RNA, 0.3 μL of each primer (10 μM),

717   and 5 μL SYBR mix in a total volume of 10 μL. Reactions were performed in

718   triplicate for each sample; three biological replicates and three reactions for each

719   biological replicate were performed. Gene expression levels were normalized to the

720   expression level of BPH *β-actin* (Chen *et al.*, 2013). The specific primers used for

721   qRT-PCR are listed in Appendix 2—table 1. The amplification conditions were as

722   follows: 95 ℃ for 5 min, followed by 45 cycles of 95 ℃ for 10 s, 60 ℃ for 20 s and

723   72 ℃ for 20 s.

724

725   **Behavioral experiments**

726   **Feeding bioassays of BPHs on artificial diet**

727   The no-choice test apparatus for evaluation of feeding decision behaviour was a BPH

728   rearing chamber and artificial diet D-97 (Figure 2A, top) (Fu *et al.*, 2001). Two layers

729   of stretched parafilm were filled with artificial diet (40 μL), either with OA (100 μM,

730   +OA) or without (-OA). BPHs (n =6-10) were placed onto the food-containing

731   parafilm at the beginning of the experiment in each of three replicates. We counted the

732   insects remaining on each parafilm (N_{on}) at 30-min intervals for 4 h. The proportion

733   of BPHs accepting food sources was calculated as (food acceptance = N_{on}/N_{total}),

734   where N_{total} represents the total number of test insects. In two-choice tests, parafilms

735   containing 40 μL of either +OA or -OA artificial diet were located at opposite open

736   ends of the chamber. Ten BPHs per replicate were introduced into the middle of the

737   cylinder at the beginning of the experiment; three replicates were performed (Figure

738   2B, top). Insects were starved for 6 h before each experiment. We scored the

739   distribution of insects on each side at 30-min intervals for 4 h. Values were totalled

740   and a position index (PI) for the 4 h period was calculated as (PI = (BPHs on the food

741   with OA - BPHs on the food without OA) / (BPHs on the food with OA + BPHs on

742   the food without OA)). The PI values range from -1 to 1, with PI = 0 indicating no

743   position preference for either control or treatment artificial diets, PI > 0 indicating

744   preference for treatment diets, and PI < 0 indicating preference for control diets. The

745   set-up was placed in a walk-in chamber at 26 ±2 ℃ at a relative humidity level of 80%

746   ±10%.

747   To directly measure feeding, we performed food choice assays as described

748   previously (Sang *et al.*, 2019; Lee *et al.*, 2010). Briefly, 10 BPHs (1-day-old

749   brachypterous female adults) were starved for 6 h and introduced into a glass

750   cylindrical column in each replicate (8≤n≤10). Then, we prepared two mixtures

751   with each non-toxic dye enclosed in parafilms and located the mixtures at opposite

752   ends of a glass cylindrical column to monitor their food preference. One mixture

753   contained the indicated concentration of OA and 10% (w/v) sucrose with blue dye

754   (Brilliant Blue FCF, 0.2 mg/ml), and the other mixture contained 2% sucrose with red

755   dye (sulforhodamine B, 0.1 mg/ml). BPHs were given 4 h to choose between these

756   two choices. After feeding, BPHs were sacrificed by freezing at -20 ℃, and then, we

757   dissected them to observe their mid-gut colors under the microscope for the presence

758   of red (N_R), blue (N_B), or purple (N_P) dye. The preference index was calculated using

759   the following equation: preference index = (N_R - N_B)/(N_R + N_B+ N_P), depending on

760   the dye/tastant combinations. Preference index of -1.0 or 1.0 indicated a complete

761   preference to either 10% sucrose with OA or 2% sucrose alone, respectively. A

762   preference index of 0.0 indicated no bias between the two food alternatives. Each

763   treatment had four biological repeats.

764   **Ingestion assay**

765   To assess whether much lower concentration of OA inhibited BPH feeding, the

766   ingestion assay was carried out following a modified protocol (Sang *et al.*, 2019).

767   After 6 h starvation, 1-day-old female BPHs were allowed to feed on 1% (w/v)

768   Brilliant Blue FCF food with or without 100 μM OA for 4 h. BPHs were sacrificed by

769   freezing at -20 ℃ after feeding. Six females were transferred into 1.5 ml centrifuge

770   tubes filled with 200 μl PBST (1× PBS with 0.2% Triton X-100) and were completely

771   ground. Then 800 μl of PBST was added and blended. Sample was centrifuged for 5

772   min at 15,871 g at 4 ℃. Subsequently, the absorbance of supernatant was measured at

773   630 nm using a NanoDrop 2000 instrument. PBST alone was used as the blank

774   control. The experiment was repeated with 4 biological replicates.

775   **Surgeries**

776   Females were anesthetized with CO_2, and the second and third antennal segments

777   were removed with a set of sharp forceps.

778   **Feeding bioassays of BPHs on rice**

779   Rice with a higher content of OA (TN1^{+OA}) was obtained by the immersion method.

780   Briefly, TN1 rice at the tillering stage was immersed in OA solution (20 mM) for 5

781   min and air-dried for 1 h. The resulting OA level was determined as follows. Firstly,

782   the rice was washed and drained, then ground to a powder using liquid nitrogen.

783   Secondly, the rice powder was placed in a 50 mL centrifuge tube and mixed with 0.5

784   mol/L HCl (fresh weight of rice : HCl = 1:5; m:m). The homogenate was placed in a

785   boiling water bath for 15–20 min then centrifuged at maximum speed. The resulting

786   supernatant was diluted 10 times with ddH$_2$O. Finally, the sample was filtered with a

787   microporous filter membrane (0.45 μm). The OA content was determined using an

788   UltiMate 3000 HPLC (Dionex Corporation, Sunnyvale, CA, USA) equipped with an

789   Agilent ZRBAX SB-C18 column (4.6 mm $\times$150 mm, 3.5 μm). The mobile phase was

790   5 mM TBA in 0.5% KH_2PO_4 (pH 2.0) with a flow rate of 1 mL/min. The eluate from

791   the column was continuously monitored at 220 nm after sample loading (5 μL).

792   To evaluate BPH food preferences across rice diets with different OA levels, we

793   performed dual choice assays as described above with the following modifications. At

794   the beginning of each experiment, ten BPHs were placed on the middle of a sponge,

795   which sealed an upside-down plastic cup containing one TN1 stem and one TN1^{+OA}

796   stem. Probing marks were detected based on a previously described method (Sogawa

797   and Pathak, 1970). In each of four replicates, BPHs (n = 4) reared on one rice stem

798   were confined for 4 h using a 50 mL polypropylene tube. The exposed plant parts

799   were stained with 1% eosin Y (Aladdin Reagent, Shanghai, China), then probing

800   marks on the plant surface were counted.

801   **Tarsal avoidance response (TAR) assay**

802   TAR assay referenced proboscis extension response (PER) assay (Lee *et al.*, 2010).

803   After BPH adults were anaesthetized with CO_2, the back of each adult was

804   immobilized on a Petri dish using a double-stick tape, while all legs were remained

805   free. BPHs were allowed to fully recover in a humidified incubator for 10-15 min.

806   Before TAR testing, water was given to BPHs to exclude insects in a fright or

807   unhealthy state, if they showed avoidance to water**.** Then, tastants were delivered to

808   the distal parts of legs without contacting the mouthpart and the antennae using a

809   small piece of Kimwipe paper wicks. TAR response of each individual was observed

810   within 3 s after tatstant treatment. The response, the hindlegs avoiding the contact of

811   Kimwipe, was counted as TAR. BPHs often adhere on wet wicks treated with water or

812   stimulant only and used leg to push away Kimwipe treated with deterrent tastants.

813   Insects were tested in a group of 15–20 individuals, and the percent of insects

814   showing TAR to each tastant was observed and recorded.

815   To determine the behavioral significance of OA to the tarsal behavior, we contacted

816   the legs of each PBH with 2% sucrose (1st exposure), 2% sucrose plus 5% OA (1st

817   exposure), 2% sucrose (2nd exposure), and 2% sucrose plus 5% OA (2nd exposure),

818   sequentially. TAR response of each individual was observed within 3 s after tatstant

819   treatment. Trials were separated by a 10 min inter trial interval so as to remove any

820   gustatory clues which could have been left behind during previous trials. To determine

821   the deterrent effect of OA, BPHs were treated with different concentrations of OA (10,

822   20, 50, 100 μM). To test the effect *NlGr23a* on OA detection via the tarsus,

823   ds*NlGr23a*-injected BPHs were applied with 100 μM OA. *GFP* dsRNA was used as a

824   control. Each treatment or control had four biological repeats.

825   **Electrical penetration graph (EPG) recording of BPH feeding behaviour**

826   BPH feeding behaviour was recorded on a Giga-8 DC EPG amplifier (GDAAS,

827   Guangdong, China) based on a previously described method (Zhang *et al.*, 2015).

828   Briefly, all experiments were carried out at $26\,℃ \pm 1\,℃$ and $70\% \pm 10\%$ relative

829   humidity under continuous light conditions. The feeding behaviour of individual

830   BPHs on liquid-diet sacs or rice was monitored for at least 3 h. The rice variety or

831   liquid-diet sacs were used alternately, and new insects were used for each recording.

832   Each treatment was replicated 5 times. The signals recorded were analysed using

833   PROBE 3.4 software (Wageningen Agricultural University, Wageningen, The

834   Netherlands). Each feeding behaviour was expressed as the duration of each

835   waveform as a proportion of total monitoring time (%) and the number of times each

836   waveform occurred.

837

838   **Tissue-specificity of *NlGr23a***

839   Antenna, mouthpart, tarsus, mid-gut, fat body, ovary and epidermis were separately

840   dissected from 20 to 30 one-day old female adults, depending on the size of the

841   organs and tissues. All collected samples were stored immediately in lysis buffer

842   offered by RNA extraction kit and ground with steel beads in a cryogenic grinder.

843   Total RNA was extracted using a Micro Elute Total RNA kit (Omega Bio-tek,

844   Norcross, GA, USA) following the manufacturer's protocols. RNA quantity was

845   determined as previously descried. Using 100 ng of total RNA, cDNA was

846   synthesized as before for a RT-PCR template. Full length gene-specific primers of

847   *NlGr23a* were used for RT-PCR analysis listed in Appendix 2—table 1. BPH *β-actin*

848   gene was used as control. PCR was performed under the following conditions: 94℃

849 for 2 min, 39 cycles of 94℃ for 30 s, 55 ℃ for 30 s, 72℃ for 90 s, and 72℃ for 5

850 min. The number of cycles was reduced to 29 for *β-actin*. PCR amplification products

851 were run on a 1.2% agarose gel.

852

853 **Statistics**

854 All statistical analyses were performed using IBM SPSS Statistics 24 (IBM, Armonk,

855 NY, USA). The differences between two groups were analysed using two-tailed *t*-test.

856 Differences among multiple groups were analysed using one-way ANOVA followed

857 by Duncan's multiple range test for multiple comparisons. *P* < 0.05 was marked "*"

858 and *P* < 0.01 was marked "**". Data were checked for normal distribution using

859 Shapiro-Wilk test.

860

861 **Acknowledgements**

867

868 **Contributions**

869 WZ designed and supervised the entire study. KK carried out ligand identification

870 experiments and feeding bioassays of BPHs on artificial diet. MZ carried out feeding

871 bioassays of BPHs on rice and TAR assays. LY performed the GC-MS and identified

872 compounds. WC helped in developing the calcium-imaging assay method. YD and

873 SX conducted the HPLC separation of the bioassay-active fractions. K. Lin performed

874 and analysed EPG recordings. K. Liu and JL carried out the quantitative RT-PCR. ZG

875 carried out microscale thermophoresis assay. KK and MZ analysed the data. WQ, MZ

876 and KK wrote the manuscript. All authors read and commented on the manuscript.

877

878 **Competing Interests**

879   The authors declare no competing interests.

880

881   **References**

882   1.   Ahn JE, Chen Y, Amrein H. Molecular basis of fatty acid taste in *Drosophila*.
883   *Elife*. 2017; 6: e30115. doi: 10.7554/eLife.30115.

884   2.   Aljunid SF, Anderson M. Ultrastructure of sensilla on the antennal pedicel of the
885   brown planthopper *Nilaparvata lugens* Stal (Insecta: Homoptera). *Cell and Tissue*
886   *Research.* 1983; 228: 313-322. doi: 10.1007/BF00204881.

887   3.   Chapman RF. Contact chemoreception in feeding by phytophagous insects.
888   *Annual Review of Entomology*. 2003; 48: 455-484. doi:
889   10.1146/annurev.ento.48.091801.112629.

890   4.   Charlu S, Wisotsky Z, Medina A, Dahanukar A. Acid sensing by sweet and bitter
891   taste neurons in *Drosophila melanogaster*. *Nature Communications*. 2013; 4:
892   2042. doi: 10.1038/ncomms3042.

893   5.   Chen J, Liang Z, Liang Y, Pang R, Zhang W. Conserved microRNAs miR-8-5p
894   and miR-2a-3p modulate chitin biosynthesis in response to 20-hydroxyecdysone
895   signaling in the brown planthopper, *Nilaparvata lugens*. *Insect Biochemistry and*
896   *Molecular Biology*. 2013; 43: 839-848. doi: 10.1016/j.ibmb.2013.06.002.

897   6.   Chen YD, Dahanukar A. Recent advances in the genetic basis of taste detection in
898   *Drosophila*. *Cellular and Molecular Life Sciences*. 2020; 77: 1087-1101. doi:
899   10.1007/s00018-019-03320-0.

900   7.   Chen W, Kang K, Lv J, Yue L, Zhang W. Galactose-*Nl*Gr11 inhibits AMPK
901   phosphorylation by activating the PI3K-AKT-PKF-ATP signaling cascade via
902   insulin receptor and Gβγ. *Insect Science*. 2021; 28: 735-745. doi:
903   10.1111/1744-7917.12795.

904   8.   Chyb S, Dahanukar A, Wickens A, Carlson JR. *Drosophila Gr5a* encodes a taste
905   receptor tuned to trehalose. *Proceedings of the National Academy of Sciences of*
906   *the United States of America*. 2003; 100: 14526-14530. doi:
907   10.1073/pnas.2135339100.

908   9.   Cook SM, Khan ZR, Pickett JA. The use of push-pull strategies in integrated pest
909   management. *Annual Review of Entomology*. 2007; 52: 375-400. doi:
910   10.1146/annurev.ento.52.110405.091407.

911   10. Dahanukar A, Lei YT, Kwon JY, Carlson JR. Two *Gr* genes underlie sugar
912   reception in *Drosophila*. *Neuron*. 2007; 56: 503-516. doi:
913   10.1016/j.neuron.2007.10.024.

914   11. Devineni AV, Sun B, Zhukovskaya A, Axel R. Acetic acid activates distinct taste
915   pathways in *Drosophila* to elicit opposing, state-dependent feeding responses.
916   *eLife*. 2019; 8: e47677. doi: 10.7554/eLife.47677.

917   12. Douglas AE. Strategies for enhanced crop resistance to insect pests. *Annual*
918   *Review of Plant Biology*. 2017; 69: 3.1-3.24. doi:
919   10.1146/annurev-arplant-042817-040248.

13. Foster S, Goodman LJ, Duckett JG. Ultrastructure of sensory receptors on the labium of the rice brown planthopper. *Cell and Tissue Research.* 1983a; 230: 353-366. doi: 10.1007/BF00213809.

14. Foster S, Goodman LJ, Duckett JG. Sensory receptors associated with the stylets and cibarium of the rice brown planthopper, *Nilapavarta lugens. Cell and Tissue Research.* 1983b; 232: 111-119. doi: 10.1007/BF00222377.

15. Freeman EG, Wisotsky Z, Dahanukar A. Detection of sweet tastants by a conserved group of insect gustatory receptors. *Proceedings of the National Academy of Sciences of the United States of America.* 2014; 111: 1598-1603. doi: 10.1073/pnas.1311724111.

16. Fu Q, Zhang Z, Hu C, Lai F, Sun Z. A chemically defined diet enables continuous rearing of the brown planthopper, *Nilaparvata lugens* (Stal) (Homoptera: Delphacidae). *Applied Entomology and Zoology.* 2001; 36: 111-116. doi: 10.1303/aez.2001.111.

17. Kang K, Yang P, Chen L, Pang R, Yu L, Zhou W, Zhu Z, Zhang W. Identification of putative fecundity-related gustatory receptor genes in the brown planthopper *Nilaparvata lugens. BMC Genomics.* 2018; 19: 970. doi: 10.1186/s12864-018-5391-5.

18. Kang K, Yue L, Xia X, Liu K, Zhang W. Comparative metabolomics analysis of different resistant rice varieties in response to the brown planthopper *Nilaparvata lugens* Hemiptera: Delphacidae. *Metabolomics.* 2019; 15: 62. doi: 10.1007/s11306-019-1523-4.

19. Karatolos N, Hatcher PE. The effect of acetylsalicylic acid and oxalic acid on *Myzus persicae* and *Aphidius colemani. Entomologia Experimentalis et Applicata.* 2008; 130: 98-105. doi: 10.1111/j.1570-7458.2008.00797.x.

20. Khan ZR, Midega CA, Pittchar JO, Murage AW, Birkett MA, Bruce TJ, Pickett JA. Achieving food security for one million sub-Saharan African poor through push-pull innovation by 2020. *Philosophical Transactions of the Royal Society of London. Series B, Biological Sciences.* 2014; 369: 20120284. doi: 10.1098/rstb.2012.0284.

21. Kim H, Kim H, Kwon JY, Seo JT, Shin DM, Moon SJ. *Drosophila Gr64e* mediates fatty acid sensing via the phospholipase C pathway. *PLoS Genetics.* 2018; 14: e1007229. doi: 10.1371/journal.pgen.1007229.

22. Lee Y, Kim S, Montell C. Avoiding DEET through insect gustatory receptors. *Neuron.* 2010; 67: 555-561. doi: 10.1016/j.neuron.2010.07.006.

23. Lee Y, Moon SJ, Montell C. Multiple gustatory receptors required for the caffeine response in *Drosophila. Proceedings of the National Academy of Sciences of the United States of America.* 2009; 106: 4495-4500. doi: 10.1073/pnas.0811744106.

24. Liman ER, Zhang YV, Montell C. Peripheral coding of taste. *Neuron.* 2014; 81: 984-1000. doi: 10.1016/j.neuron.2014.02.022.

25. Massonie G. Breeding of a biotype of *Myzus persicae Sulzer* on a synthetic medium. V. Influence of oxalic and gentisic acids on the nutritive value of a synthetic medium. *Annales De La Nutrition Et De L'alimentation.* 1980; 34: 139-146.

26. Moon SJ, Kottgen M, Jiao Y, Xu H, Montell C. A taste receptor required for the caffeine response *in vivo*. *Current Biology*. 2006; 16: 1812-1817. doi: 10.1016/j.cub.2006.07.024.

27. Nelson G, Hoon MA, Chandrashekar J, Zhang YF, Ryba NJP, Zuker CS. Mammalian sweet taste receptors. *Cell*. 2001; 106: 381–390. doi: 10.1016/s0092-8674(01)00451-2.

28. Ozaki K, Ryuda M, Yamada A, Utoguchi A, Ishimoto H, Calas D, Yoshikawa H. A gustatory receptor involved in host plant recognition for oviposition of a swallowtail butterfly. *Nature Communications*. 2011; 2: 542. doi: 10.1038/ncomms1548.

29. Poudel S, Kim Y, Kim YT, Lee Y. Gustatory receptors required for sensing umbelliferone in *Drosophila melanogaster*. *Insect Biochemistry and Molecular Biology*. 2015; 66: 110-118. doi: 10.1016/j.ibmb.2015.10.010.

30. Poudel S, Kim Y, Kwak JS, Jeong S, Lee Y. Gustatory receptor 22e is essential for sensing chloroquine and strychnine in *Drosophila melanogaster*. *Insect Biochemistry and Molecular Biology*. 2017; 88: 30-36. doi: 10.1016/j.ibmb.2017.07.007.

31. Prokopy RJ, Collier RH, Finch S. Leaf color used by cabbage root flies to distinguish among host plants. *Science*. 1983; 221: 190-192. doi: 10.1126/science.221.4606.190.

32. Rimal S, Sang J, Poudel S, Thakur D, Montell C, Lee Y. Mechanism of acetic acid gustatory repulsion in *Drosophila*. *Cell Reports*. 2019; 26: 1432-1442.e4. doi: 10.1016/j.celrep.2019.01.042.

33. Robertson HM, Wanner KW. The chemoreceptor superfamily in the honey bee, *Apis mellifera*: Expansion of the odorant, but not gustatory, receptor family. *Genome Research*. 2006; 16: 1395-1403. doi: 10.1101/gr.5057506.

34. Sang J, Rimal S, Lee Y. Gustatory receptor 28b is necessary for avoiding saponin in *Drosophila melanogaster*. *EMBO Reports*. 2019; 20: e47328. doi: 10.15252/embr.201847328.

35. Sato K, Tanaka K, Touhara K. Sugar-regulated cation channel formed by an insect gustatory receptor. *Proceedings of the National Academy of Sciences of the United States of America*. 2011; 108: 11680-11685. doi: 10.1073/pnas.1019622108.

36. Scott K. Gustatory processing in *Drosophila melanogaster*. *Annual Review of Entomology*. 2018; 63: 15-30. doi: 10.1146/annurev-ento-020117-043331.

37. Shim J, Lee Y, Jeong YT, Kim Y, Lee MG, Montell C, Moon SJ. The full repertoire of *Drosophila* gustatory receptors for detecting an aversive compound. *Nature Communications*. 2015; 6: 8867. doi: 10.1038/ncomms9867.

38. Sogawa K, Pathak MD. Mechanisms of brown planthopper resistance in Mudgo variety of rice (Hemiptera: Delphacidae). *Applied Entomology and Zoology*. 1970; 5: 145-158. doi: 10.1303/aez.5.145.

39. Sogawa K. The rice brown planthopper: feeding physiology and host plant interactions. *Annual Review of Entomology*. 1982; 27: 49-73. doi: 10.1146/annurev.en.27.010182.000405.

40. Stanley M, Ghosh B, Weiss ZF, Christiaanse J, Gordon MD. Mechanisms of lactic acid gustatory attraction in *Drosophila*. *Current Biology*. 2021; 31: 3525-3537.e6. doi: 10.1016/j.cub.2021.06.005.

41. Sun L, Hou W, Zhang J, Dang Y, Yang Q, Zhao X, Ma Y, Tang Q. Plant metabolites drive different responses in caterpillars of two closely related *Helicoverpa* species. *Front Physiology*. 2021; 12: 662978. doi: 10.3389/fphys.2021.662978.

42. Wienken CJ, Baaske P, Rothbauer U, Braun D, Duhr S. Protein-binding assays in biological liquids using microscale thermophoresis. *Nature Communications*. 2010; 1: 100. doi: 10.1038/ncomms1093.

43. Wu B, Huang S, Li C, Sun Z, Zhou J, Ling Y, Jiang X, Huang X, Long L, Huang F. Effect of environmental factor on secondary substances of rice planting and relationship with resistance to brown planthopper (Homoptera: Delphacidae). *Southwest China Journal of Agricultural Sciences*. 2016; 29: 2371-2378.

44. Xu W, Papanicolaou A, Zhang H, Anderson A. Expansion of a bitter taste receptor family in a polyphagous insect herbivore. *Scientific Reports*. 2016; 6: 23666. doi: 10.1038/srep23666.

45. Yang J, Guo H, Jiang NJ, Tang R, Li GC, Huang LQ, van Loon JJA, Wang CZ. Identification of a gustatory receptor tuned to sinigrin in the cabbage butterfly *Pieris rapae*. 2021; *PLoS Genetics*. 17: 7 e1009527. doi: 10.1371/journal.pgen.1009527.

46. Yoshihara T, Sogawa K, Pathak MD, Juliano BO, Sakamura S. Oxalic acid as a sucking inhibitor of the brown planthopper in rice (Delphacidae, Homoptera). *Entomologia Experimentalis et Applicata*. 1980; 27: 149-155. doi: 10.1007/BF00573889.

47. Zhang G, Zhang W, Lian B, Gu L, Zhou Q, Liu TX. Insecticidal effects of extracts from two rice varieties to brown planthopper, *Nilaparvata lugens*. *Journal of Chemical Ecology*. 1999; 25: 1843-1853. doi: 10.1023/A:1020981716293.

48. Zhang HJ, Anderson AR, Trowell SC, Luo AR, Xiang ZH, Xia QY. Topological and functional characterization of an insect gustatory receptor. *PLoS One*. 2011; 6: e24111. doi: 10.1371/journal.pone.0024111.

49. Zhang Z, Cui B, Zhang Y. Electrical penetration graphs indicate that tricin is a key secondary metabolite of rice, inhibiting phloem feeding of brown planthopper, *Nilaparvata lugens*. *Entomologia Experimentalis et Applicata*. 2015; 156: 14-27. doi: 10.1111/eea.12307.

50. Zindler-Frank E. Oxalate biosynthesis in relation to photosy nthetic pathway and plant productivity: a survey. *Zeitschrift Für Pflanzenphysiologie*. 1976; 80: 1-13. doi: 10.1016/S0044-328X(76)80044-X.